PHILOSOPHICAL TRANSACTIONS OF THE ROYAL SOCIETY A MATHEMATICAL, PHYSICAL & ENGINEERING SCIENCES

Quaternary Elevation Change of the Gulf of Corinth in Central Greece

Rob Westaway

Phil. Trans. R. Soc. Lond. A 1996 **354**, 1125-1164
doi: 10.1098/rsta.1996.0043

Quaternary elevation change of the Gulf of Corinth in central Greece

By Rob Westaway

16 Neville Square, Durham DH1 3PY, UK

Contents

Dramatic elevation changes have occurred since early Pleistocene time in and around the Gulf of Corinth sedimentary basin in central Greece, which is actively extending at a maximum rate of *ca.* 2 mm a^{-1}. Shoreline deposits younger than 1 million years are found at up to *ca.* 1200 m elevation south of the Gulf, with sediment from an older Plio-Pleistocene basin above 1750 m. The Gulf floor, in the hanging-wall of normal faults along its southern coast, has subsided up to *ca.* 1650 m on the same timescale. However, other hanging-wall localities such as the Corinth isthmus – east of the Gulf – have uplifted instead. During the past million years the Gulf has alternated between marine and lacustrine environments in response to glacially induced sea-level variations. This study establishes its chronology of marine and lacustrine terraces for the past half million years, allowing lateral variations in uplift to be investigated. To explain the observed elevation changes, it is suggested that *ca.* 0.9 million years ago the previously lacustrine Gulf became flooded by *ca.* 80 m during an interglacial marine highstand. The resulting *ca.* 0.8 MPa increase in lithostatic pressure at the base of the brittle upper crust caused southward lower-crustal flow to beneath the older Plio-Pleistocene basin. Isostatic adjustment uplifted this basin, creating unstable topography that enabled rapid erosion. This lower-crustal flow,

Phil. Trans. R. Soc. Lond. A (1996) **354**, 1125–1164
Printed in Great Britain

which since been maintained by the sediment load in the Gulf that results from this erosion, also causes the hanging-wall uplift of the Corinth isthmus and other 'anomalous' localities. The Gulf of Corinth is thus an important case study locality for revealing the existence of lower-crustal flow during continental extension.

1. Introduction

The Gulf of Corinth extensional sedimentary basin in central Greece is near the western margin of the Aegean extensional province. Uplift of its surroundings is revealed by late Pleistocene coastal sediments above 1200 m elevation (Ori 1989), and uplifted beaches and notches in limestone coasts (Jackson *et al.* 1982). The excellent exposures of sediments and active nomal faults make this basin an important natural laboratory for testing models of continental extension.

Recent work has highlighted the importance of lower-crustal flow in regulating the isostatic equilibrium of extensional basins (Wernicke 1990; Kruse *et al.* 1991). In the absence of significant sedimentation, this flow will be inward, to beneath a region that is extending. However, with a substantial sedimentation rate it may instead be outward, to beneath the surroundings of a depocentre (Westaway 1994*a*). Outward lower-crustal flow has been significant during the Quaternary evolution of extensional basins in western Turkey, near the eastern margin of the Aegean (Westaway 1994*b*). Western Turkey experiences low rates of denudation (typically less than *ca.* 0.1 mm a^{-1}) over a broad area, with sediment being transported by rivers over distances of up to several hundred kilometres to coastal depocentres where sedimentation rates are up to *ca.* 1 mm a^{-1} (Westaway 1994*b*). This westward flux of sediment is balanced by eastward flow of lower-crustal material. Although western Turkey is actively extending, the rate is low (no more than a few tenths of 1 mm a^{-1} on any individual normal fault zone), such that the elevation changes due to isostatic compensation of sedimention are much faster than those due to faulting (Westaway 1994*b*). Finally, at the base of the brittle layer, the estimated excesses of lithostatic pressure beneath the depocentres offshore of western Turkey are small compared with the pressure changes caused by interglacial sea-level variations (Westaway 1994*b*), suggesting that changes in sedimentary environments during Pleistocene time may be explained.

The Gulf of Corinth is rather different from the sedimentary basins in western Turkey: its extension rate is much faster, sediment transport distances are no more than a few tens of kilometres, and Quaternary denudation rates in some surrounding localities have been high (Ori 1989). However, here also there is evidence for a dramatic change in basin form in early Pleistocene time (Ori 1989). By analogy with western Turkey, this may be evidence for a change in the sense of lower-crustal flow, possibly resulting from lithostatic pressure variations induced by interglacial sea-level variations. This study thus reappraises the Gulf of Corinth using the copious published data, much of which has been confirmed first hand during field visits between 1982 and 1988. Its aim is to quantify rates and durations of elevation change and to assess their cause. A major objective is to investigate whether the apparently anomalous pattern of elevation changes can indeed be explained by flow in the lower crust.

The Corinth region has witnessed three major controversies. The first concerns the

PHILOSOPHICAL TRANSACTIONS OF THE ROYAL SOCIETY A MATHEMATICAL, PHYSICAL & ENGINEERING SCIENCES

Table 1. *Glacio-eustatic global marine highstands*

(Stage denotes stage of the oxygen isotope timescale, and h and t are sea-level and its timing, adapted from Westaway (1993*b*). The highstands between stages 13 and 25 are compatible with Shackleton (1987) and Shackleton *et al.* (1990). The 3a highstand 50 000 years ago is compatible with Chappell & Shackleton (1986). For the early Holocene highstand I adopt +2 m as the highest water level allowing for wave and tidal action, and +1.5 m as the highest mean water level. In the absence of tectonic elevation changes, limestone notches are thus expected at +1.5 m but sediments are expected at up to +2 m.)

stage	t/ka	h/m	label	event name	terrace name
25	900	0	25	Emilian	
23	870	−30	23		
21	820	−10	21		
19	780	−10	19		
17	700	−10	17		
15	620	−10	15		
13	520	−10	13		
11	460	0	11	Sicilian	Veliniatika
9	360	0	9e		Fortikia/Nicoletto/Megali Lakka
	330	−10	9c		
	300	−30	9a		
7	250	−5	7e	Palaeotyrrhenian	Temple
	230	−5	7c		Ancient Corinth
	200	−25	7a		Tripos
5e	125	+3	5e	Eutyrrhenian	New Corinth
5c	100	−15	5c		Kounoukles
5a	80	−15	5a		Agios Spiridon
3c	60	−30	3c		
3a	50	−35	3a		
1	7	+2	1	Holocene	

interpretation of scarps in the landscape. Vita-Finzi & King (1985) dismissed the long history of marine terrace studies, claiming that most scarps south of the Gulf are normal fault scarps. Keraudren & Sorel (1987) later published a detailed chronology of marine terraces, which Doutsos & Piper (1990) reinterpreted as a faulted sequence of fewer terraces. Faulted terrace sequences are often difficult to interpret: compare, for instance, the results of Ghisetti (1992) and Valensise & Pantosti (1992) for the coasts of the Messina Strait in southern Italy. Having investigated this locality and other terrace sequences in Italy (Westaway 1993*b*), and having thus related the glacio-eustatic chronology of the Mediterranean region to the standard oxygen isotope timescale (OIT) (table 1), it now appears feasible to resolve this controversy in the Gulf of Corinth.

The second controversy concerns dating. Methods used in the past include faunal associations, which may in fact be environmentally determined (Vita-Finzi & King 1985; Collier *et al.* 1992). Using radiocarbon dating, Vita-Finzi & King (1985) dated to *ca.* 7000 years ago fossils in an ancient canal cut, although civilization in Greece is

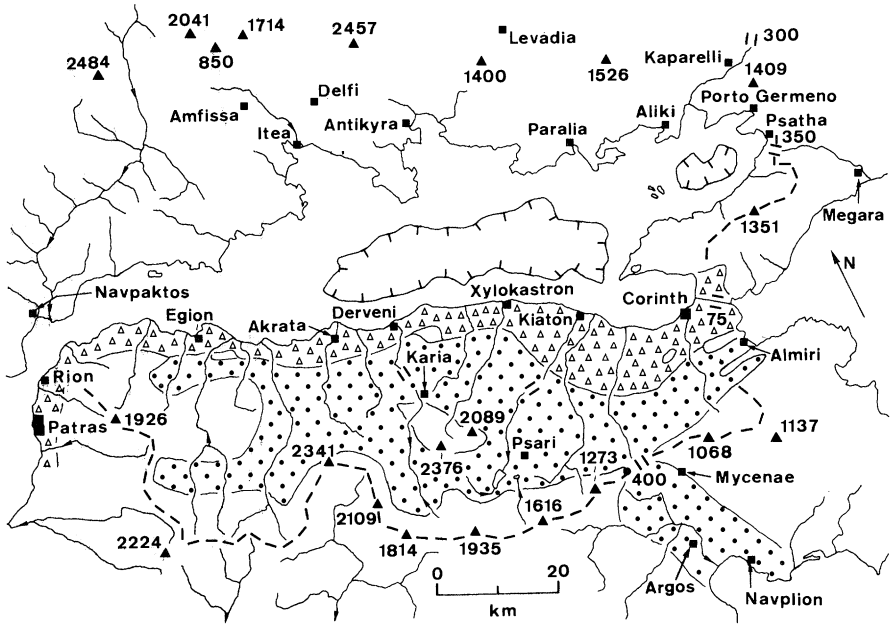

Figure 1. Location map, showing topography, bathymetry, drainage, and simplified geology for the present-day Gulf of Corinth extensional basin and the surrounding Plio-Pleistocene basins. Lines with inward-facing ticks surround the abyssal plains, at *ca.* 800 m in the Gulf of Corinth and *ca.* 350 m in the Alkyonides Gulf. Dashes indicate the present-day drainage divide south of the Gulf of Corinth, separating rivers that drain internally or into the Gulf from those that drain southward. Dots indicate outcrop of the fluvio-lacustrine Plio-Pleistocene Proto Gulf of Corinth basin (PGCB). Open triangles denote outcrop of upper Pleistocene raised shorelines south of the Gulf of Corinth. In the Argos basin in the southeastern part of the figure, PGCB sediment, uplifted marine terraces, and sediment of the modern fluvial delta plain are undifferentiated. Double lines indicate present-day drainage divides created by flow reversal along rivers south of the Gulf, caused by lateral variations in uplift, or other cols with altitudes in metres. Note that the continuity between the PGCB sediment and the Saronic Gulf south of the Corinth isthmus at Almiri probably does not indicate an eastward outlet to the PGCB: the adjoining sea area has probably subsided recently in the hanging-wall of nearby normal faults.

no older than *ca.* 5000 years (*ca.* 3000 B.C.) (Kinder & Hilgemann 1974, p. 47). The influx of eroded calcareous sediment enriches Gulf of Corinth water in ^{12}C, causing a low $^{14}C/^{12}C$ ratio (Heezen *et al.* 1966) that may explain this systematic error. Other radiocarbon dating by Vita-Finzi & King (1985) and Vita-Finzi (1987) instead gave *ca.* 30 000 year ages for many localities that other studies have claimed are much older, possibly because samples were recrystallized or otherwise contaminated with modern carbon (Collier *et al.* 1992). Uranium series dates now available may enable this controversy to also be resolved.

The third controversy involves the measurement and interpretation of elevation changes around the Gulf. Limestone notches along its coasts form at sea-level, mainly through abrasion by molluscs (Leeder *et al.* 1991). In many localities these notches are now found above sea-level. The first aspect of this controversy concerns the validity of the assumption that they are Holocene and indicate absolute tectonic uplift since the present sea-level stabilized. Although many studies have argued this (Jackson *et al.* 1982; Roberts & Jackson 1991), most notches discussed are within 1–2 m of present-day sea-level. The Mediterranean sea-level has been stable to within a

few tens of centimetres over the past 4000 years or so (Flemming 1978; Flemming & Webb 1986), but stood at *ca.* +2 m around 6–7000 years ago (Westaway 1993*b*). Furthermore, the sea-level was probably *ca.* +3 m during OIT stage 5e, 125 000 years ago (Shackleton 1987). Elsewhere in the Mediterranean region notches are known that evidently record this event and earlier Late Pleistocene interglacial marine high-stands (Flemming 1965, 1968). The second aspect concerns discrepancies between observed elevation changes and predictions based on conventional models for the isostatic response to active normal faulting. In a region such as the Gulf of Corinth that is extending coseismically by slip in normal-faulting earthquakes, the instantaneous coseismic hanging-wall subsidence is *ca.* 5–10 times larger than the footwall uplift. However, interseismic relaxation cancels some hanging-wall subsidence and adds to the footwall uplift, such that over each earthquake cycle they are more nearly equal (King *et al.* 1988). Many footwall localities in the Gulf are uplifting, and many hanging-wall localities are subsiding, as is expected. Anomalies include the Corinth isthmus, a hanging-wall locality that has uplifted more than 150 m since early Pleistocene time (Collier & Dart 1991). Furthermore, uplift south of the Gulf persists beyond the *ca.* 10 km expected dimensions of isostatic footwall uplift beside normal faults. Arbitrary past explanations for 'anomalous' uplift around the Gulf have included local shortening (Mariolakos & Stiros 1987), magmatism (Collier 1990), and the isostatic response to subduction of sediment beneath the Aegean (Le Pichon & Angelier 1981). The marine terrace controversy has previously restricted the extent to which uplift around the Gulf has been resolved.

This study, first, summarizes background information from past studies of the Gulf of Corinth. Second, markers of marine and lacustrine palaeoshorelines are described and interpreted given the available absolute dating evidence and the known history of interglacial sea-level variations. Finally, the overall isostatic equilibrium and horizontal fluxes of material into and out of this basin are addressed.

2. Background information

(*a*) *The Gulf of Corinth basin*

The Gulf of Corinth extensional basin is an ESE-trending arm of the Ionian Sea, with length *ca.* 120 km and surface area *ca.* 2300 km^2 (figure 1). It reaches the open sea in the west, through the 2 km wide and 55 m deep Rion strait. It is separated from the Saronic Gulf to the east by the 6 km wide and up to 90 m high Corinth isthmus, where a ship canal has been cut. Its eastern end has two arms: the Lecheon Gulf (which adjoins the isthmus, and is up to *ca.* 200 m deep) and the Alkyonides Gulf, separated by the Perachora peninsula.

The earliest Aegean extension began around 15–20 million years ago (see compilation of estimates by Westaway (1993*a*)). However, there is little evidence for Miocene extension in central Greece. Most, if not all, of its extension has thus occurred since the start of Pliocene time, *ca.* 5 million years ago (Roberts & Jackson 1991). Earthquake slip vectors and striations on normal faults indicate that the Gulf is extending southward (Roberts & Jackson 1991). Although some of its north coast is normal-fault bounded (Roberts & Jackson 1991), the southward tilt of its floor (Brooks & Ferentinos 1984) indicates that the active normal faults at its south coast are more important. Other active normal faults occur up to *ca.* 20 km farther south (Doutsos & Piper 1990).

PHILOSOPHICAL TRANSACTIONS OF THE ROYAL SOCIETY A MATHEMATICAL, PHYSICAL & ENGINEERING SCIENCES

(i) *Active sedimentation and erosion*

For *ca.* 60 km WNW of the Perachora peninsula, the Gulf is *ca.* 30 km wide. This central part is bounded to the south, beyond a *ca.* 5–10 km wide zone of uplifted late Pleistocene coastal sediment, by a *ca.* 15–20 km wide older Plio-Pleistocene basin (figure 1). For *ca.* 45 km WNW of the Perachora peninsula, the Gulf floor contains a *ca.* 10 km wide 'abyssal plain' at 430–470 fathoms (*ca.* 790–860 m) depth (Heezen *et al.* 1966). Farther west, this floor rises gently to 250 fathoms (*ca.* 460 m) at the western end of the wide part of the Gulf. The eastern Alkyonides Gulf has a *ca.* 50 km^2 abyssal plain at *ca.* 350 m depth, bounded to the west by shallows at *ca.* 300 m. These abyssal plains form depocentres for turbidites (Brooks & Ferentinos 1984; Ferentinos *et al.* 1988), transported to the Gulf from the south by rivers that are eroding the uplifted Plio-Pleistocene sediment (figure 1). The south coast of the Gulf contains active fan deltas above foreset sequences that reach to the abyssal plain (Ori 1989). Some rivers now flow SSW in the southern part of this uplifted basin, having reversed their flow direction in the recent past (figure 1) (Dufaure *et al.* 1975). They thus indicate SSW tilting, suggesting a SSW taper in uplift beyond the Gulf's immediate surroundings. A seismic reflection profile between Xylokastron and Paralia indicates that the turbidites are up to 1 km thick beneath the *ca.* 900 m deep abyssal plain (Brooks & Ferentinos 1984). However, they thin northward and are absent from the shallow northern parts of the Gulf.

(ii) *Relationship between the Modern Gulf and the Plio-Pleistocene basin*

The Plio-Pleistocene basin, called the proto-Gulf-of-Corinth basin (PGCB) by Ori (1989), was very different from the modern Gulf. It was shallow, closed to the west (Ori 1989), and in Pliocene time was isolated from the Saronic Gulf near the Corinth isthmus (Collier & Dart 1991). Its fluvial and lacustrine sediment indicates axial drainage to the ESE (Ori 1989). The continuous sediment (Ori 1989) suggests that the PGCB drained southeastward into the Gulf of Argos (figure 1), the drainage divide between the modern Gulfs being now at *ca.* 400 m elevation.

A seismic reflection profile from Derveni to Itea (Myrianthis 1984) is interpreted with the base of the water column at 1.1 s two-way time and base Pliocene at up to 2.2 s. With the seismic wave velocity 1.4 km s^{-1} in water and 2.5 km s^{-1} in sediment, this means a water depth of 800 m and a sediment thickness of 1.4 km. A profile (Q in figure 2) from Kiaton to Antikyra (Myrianthis 1984) is interpreted with the base of sediment at up to 3.5 s, with a sediment thickness of *ca.* 3 km. With 1 km of turbidites, the estimated thicknesses of PGCB sediment are thus *ca.* 0.4 km and *ca.* 2 km in these two localities. Brooks *et al.* (1988) determined the maximum free-air gravity anomaly in the Gulf as −65 mgal. They explained this as the effect of the water column plus 1.2 km of sediment with a density contrast of −450 kg m^{-3}, indicating a *ca.* 0.2 km maximum thickness of PGCB sediment. It is thus unclear whether Ori's (1989) suggestion, that most of the Gulf is underlain by thick PGCB sediment, is correct. However, a profile from Kiaton to Paralia (P), just west of the Alkyonides Gulf, shows turbidites overlying basement around locality P1 in figure 2 (Brooks & Ferentinos 1984). The Alkyonides Gulf was thus not part of the PGCB.

Ori (1989) interpreted a widespread mid-Pleistocene conglomerate as marking the last PGCB sedimentation before the present phase began. Mammal fossils date it to Calabrian age (1.6–0.9 million years ago) (Symeonides *et al.* 1987), like the youngest PGCB lacustrine sediment (Kelletat *et al.* 1976). The present phase of sedimentation

PHILOSOPHICAL TRANSACTIONS OF THE ROYAL SOCIETY A MATHEMATICAL, PHYSICAL & ENGINEERING SCIENCES

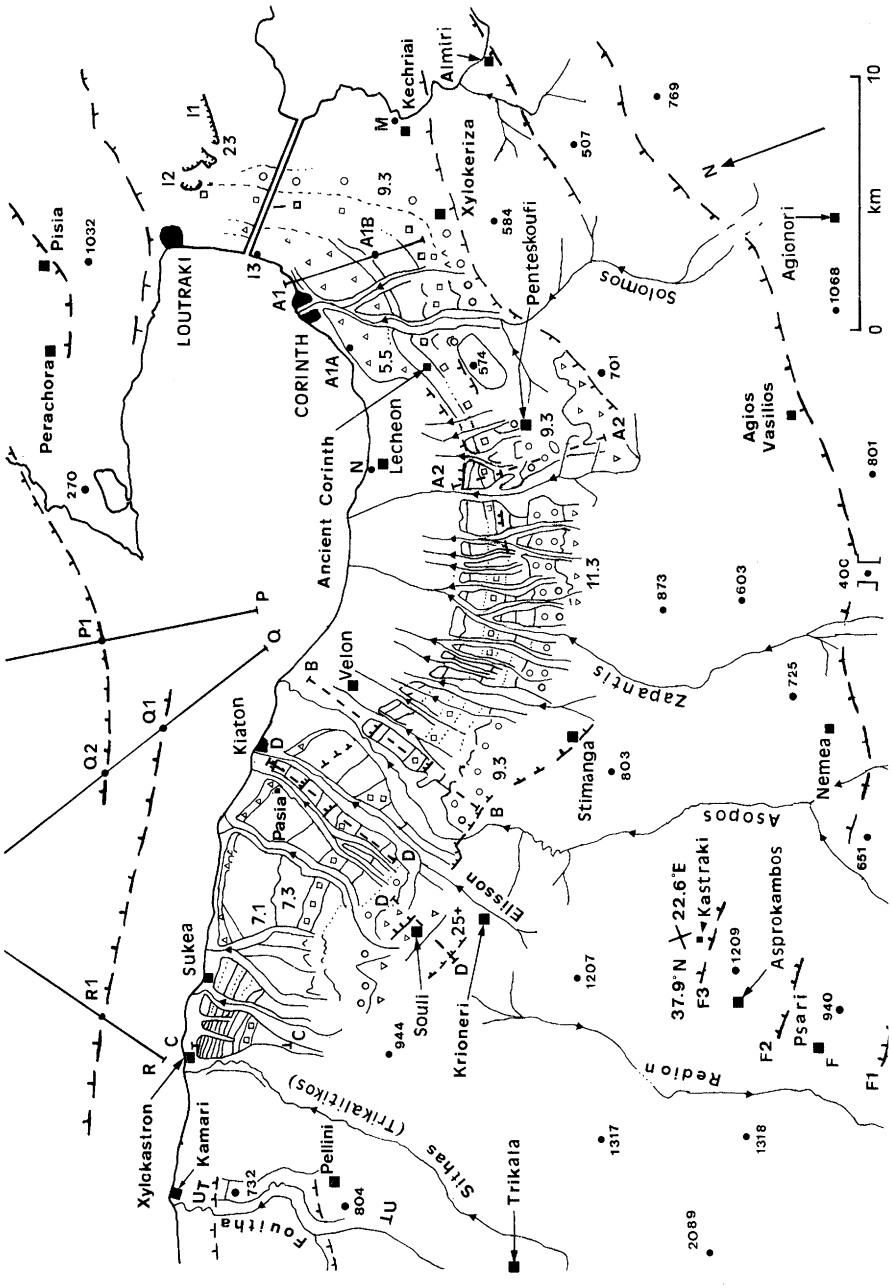

Figure 2. Map of the Gulf of Corinth coastline between Corinth and Xylokastron, showing active normal faults and marine and lacustrine terraces. Localities A1, A2, B, C, D, F, I, P, Q, R, and U are indicated. To facilitate identification, terraces 5.5, 7.5, 9.3 and 11.3 are labelled with upward pointing triangles, squares, circles, and downward pointing triangles, respectively. Detail northeast of the Corinth canal is omitted (see figure 3). Significant normal faults are shown with hanging-wall ticks; the symbol follows the base of the footwall escarpment.

thus began around 0.9 million years ago. This roughly matches the timing of a marine incursion through the Corinth isthmus (Collier & Dart 1991), which presumably occurred during the marine highstand of OIT stage 25 around 0.9 million years ago. The Corinth isthmus most likely regulated the lake level in the PGCB during early Pleistocene time. Its estimated −80 m elevation (from the modern altitudes of *ca.* 75 m for the isthmus and *ca.* 155 m for the marine terrace that formed 0.9 million years ago, from Collier & Dart (1991)) indicates the lake level more than 0.9 million years ago.

The amount of uplift of the PGCB has also been debated: values suggested range from *ca.* 2000 m (Kelletat *et al.* 1978; Keraudren & Sorel 1987) and *ca.* 1500 m (Stiros 1986; Ori 1989) to *ca.* 600–800 m (Doutsos & Piper 1990). The highest PGCB sediment of which I am aware covers mount Mavron, south of Derveni, whose 1757 m summit is in the footwall of a major normal fault. PGCB sediment *ca.* 10 km farther south at Karia, near the southern margin of the basin, is at *ca.* 1200 m. The highest late Pleistocene coastal sediment is at *ca.* 900–1200 m, at Evrostini, north of Mavron (Ori 1989). With the lake level at −80 m before 0.9 million years ago, I thus suggest *ca.* 1837 m as the maximum demonstrable uplift south of the central Gulf, at a time-averaged rate of *ca.* 2 mm a^{-1}.

Three major changes in the form of the Gulf have thus occurred since deposition of the PGCB: the marine connection was first established across the Corinth isthmus; second, a connection with the Ionian Sea developed through the Rion strait; and third, the Corinth isthmus rose above sea-level. These connections only existed during interglacial marine highstands. At times of lower sea-lavel, the Gulf has formed a brackish lake (Doutsos & Piper 1990) whose level is regulated at whichever end is lower.

(iii) *Geodetic measurements*

Attempts have been made to measure the extension rate across the Gulf of Corinth, using modern surveying methods to remeasure distances between points that were first surveyed about a century ago (Billiris *et al.* 1991; Le Pichon *et al.* 1994, 1995). Both studies reported extension rates of *ca.* 10 mm a^{-1} across the Gulf, and Le Pichon *et al.* (1994) deduced that this extension is fastest, at *ca.* 15 mm a^{-1}, at its western end. This conflicts with the geological evidence (see below). No attempt is made here to explain these results, as previous experience (Westaway 1994*b*) indicates that geodetic studies in the Aegean region can yield apparent deformation rates that are much too fast to be sustainable over geological timescales. Future geodetic measurements, which may be better constrained, may thus provide an independent test of the extension rates calculated here from geological evidence.

(*b*) *Marine terraces and Pleistocene sea-level variations*

Many early studies of Mediterranean terraces disregarded tectonic elevation changes, and thus expected the same sequence at all localities, with heights directly related to palaeo-water-level. An early scheme (Zeuner 1956), using offset palaeoshorelines at Monastir in Tunisia, called the three youngest Pleistocene terrace-forming events Epi-, Late-, and Main-Monastirian. Many early studies thus interpreted terraces solely by counting upwards, believing that the third and fourth Pleistocene terraces above sea-level are always Main-Monastirian (or Eutyrrhenian) and Palaeotyrrhenian. However, because the sea-level differs between highstands, the terrace sequence in any locality depends on its uplift rate (Westaway 1993*b*). This past approach is therefore wrong in principle, and many published interpretations thus have no basis. The coastline at Monastir is now known anyway to consist of a single Eutyrrhenian terrace that is offset by active faults (Paskoff & Sanlaville 1981). The 'Milazzian' is another Quaternary stratigraphic term that is also now meaningless: its 'stratotype' at Milazzo in Sicily now appears to have formed during OIT stage 5e (125 ka) (Hearty *et al.* 1986; Westaway 1993*b*), not during a separate highstand. I adopt the +3-m sea-level during stage 5e from Shackleton (1987).

I designate the stage 7 and 9 highstands (250 000 and 360 000 years ago) as 7e and

PHILOSOPHICAL TRANSACTIONS OF THE ROYAL SOCIETY A MATHEMATICAL, PHYSICAL & ENGINEERING SCIENCES

9e. There is evidence for a terrace in southern Italy between 5e and 7e, which I call 7a (200 000 years ago; sea-level *ca.* −25 m), plus at least one other terrace-forming event between 7e and 9e (Westaway 1993*b*). Oxygen isotope variations suggest two such events (Collier *et al.* 1991, fig. 2), which I interpret as 300 000 (sea-level −30 m) and 330 000 years ago (−10 m). Stage 7 has a double peak in sea-level, whose first part is my 7e event; I call the second peak (at 230 000 years ago) 7c. The sea was probably below its present level at these times (Shackleton 1987), at *ca.* −5 m. Recognition of the *ca.* 2 m early Holocene sea-level, and of the many glacio-eustatic terrace-forming events over the past 500 000 years or so, with different palaeo-water-levels (table 1), is essential for understanding marine terraces in the Gulf of Corinth. Other lacustrine shorelines are also expected from times of reduced sea-level.

3. Quaternary elevation changes in the Gulf of Corinth

(*a*) *Past investigations of marine terraces*

Pleistocene marine terraces are found along uplifting coasts of the Gulf of Corinth (Depéret 1913; Mitzopoulos 1933; Schröder 1970, 1975; Keraudren 1970, 1971, 1972; Freyberg 1973; Dufaure *et al.* 1975; Sauvage & Dufaure 1976; Kelletat *et al.* 1976, 1978; Sébrier 1977; Herforth & Richter 1979; Richter *et al.* 1979; Keraudren & Sorel 1987). However, its south coast is also cut by active normal faults (Doutsos & Piper 1990), so terrace scarps and fault scarps are both present. This locality was first studied by Depéret (1913), who reported a single faulted terrace. Keraudren (1970, 1971, 1972) established that some of the stepped terrace surfaces between Kiaton and Souli are stratigraphically distinct. Dufaure *et al.* (1975), Schröder (1975), Kelletat *et al.* (1976), Sébrier (1977), Herforth & Richter (1979) and Richter *et al.* (1979) interpreted a range of different terrace ages, both in this locality and elsewhere in the Gulf, although some results were inconsistent. Vita-Finzi & King (1985) suggested instead that almost all scarps between Kiaton and Souli are normal fault scarps.

Following mapping by Dufaure & Zamanis (1980), Keraudren & Sorel (1987) made a detailed interpretation with up to 15 terraces since 250 000 years ago. Their numbering scheme was linked to the OIT, such that for example 7.1 means the youngest stage 7 terrace. Eight Pleistocene terraces are identified in the lowest *ca.* 600 m of the Kiaton-Souli section, the terrace above *ca.* 600 m at Souli being interpreted with an age of *ca.* 460 000 years (stage 11). Their scheme uses constraints from both the Corinth and Kiaton-Souli areas, and thus requires terraces to be correlated unambiguously between these localities. The constraints are, first, the warm-water gasterpod *Strombus bubonius*, diagnostic of the Eutyrrhenian, is found in the New Corinth terrace. Second, nannoplankton in foresets of the *ca.* 600 m terrace at Souli is from chronozone NN20, which begins during OIT stage 12. This requires this *ca.* 600 m terrace to be no older than stage 11. Third, uranium series dates from near Corinth indicate ages of 49 000 ± 20 000 years for the New Corinth terrace and 235 000 + 40 000/ − 30 000 years for the Ancient Corinth terrace (see Sébrier 1977). The Keraudren & Sorel (1987) interpretation of the New Corinth terrace (5.5 is stage 5e or 125 000 years) is inconsistent with this date. Their interpretation of the Ancient Corinth terrace (7.3 is stage 7c or *ca.* 230 000 years ago) is non-unique, as the uncertainty in its date spans several terrace-forming events (table 1).

Doutsos & Piper (1990) reinterpreted the Kiaton-Souli section with only four terraces up to *ca.* 660 m (from stages 5, 7, 9, and 11) plus many fault scarps. They

PHILOSOPHICAL TRANSACTIONS OF THE ROYAL SOCIETY A MATHEMATICAL, PHYSICAL & ENGINEERING SCIENCES

Table 2. *Holocene coastal elevation changes*

(Localities J, K, M, and N are archaeological sites; L is an uplifted limestone notch, which presumably dates from the early Holocene highstand. For information see references in Vita-Finzi & King (1985) (J and K), Leeder *et al.* (1991) (L), and Flemming (1978) (M and N). H is present-day elevation above sea-level, t is age, D is sea-level at time of formation, and U is uplift rate estimated as $(H - D)/t$.)

locality	label	H/m	t/ka	D/m	U/(mm a^{-1})
Aliki	J	−2.0	2.4	0	−0.83
Porto Germeno	K	−1.5	2.4	0	−0.63
Psatha	L	2.0	7.0	+1.5–+2	0.00–0.07
Kenchriai	M	−2.0	2.5	0	−0.80
Lecheon	N	−0.7	2.0	0	−0.35

thus disputed several terraces identified previously. For instance, the scarp at *ca.* 200 m above the 'terrace' that was regarded as 'Milazzian' by Keraudren (1970, 1971, 1972), was disregarded by Kerauderen & Sorel (1987), but was interpreted as a fault scarp (fault F10) offsetting a Palaeotyrrhenian terrace by Doutsos & Piper (1990). Because Keraudren & Sorel's (1987) scheme requires that terraces be correlated from Kiaton-Souli to Corinth, its validity is thus questioned.

(*b*) *Elevation changes*

This section investigates elevation changes around the eastern two thirds of the Gulf, in the light of these observations. The western third of the Gulf is not documented in as much detail (see, for example, Doutsos *et al.* 1985; Roberts & Jackson 1991). However, because extension there is expected to be slower than farther east (Ori 1989), the localities considered cover the maximum rates of elevation change.

(i) *Locality I: Corinth canal*

The Corinth canal cut (figure 2) has been documented by Collier (1990) and Collier & Dart (1991). Five late Pleistocene coastal sequences overlie the Pliocene to lower Pleistocene 'Corinth Marl' of Freyberg (1973). Collier *et al.* (1992) dated the fourth coastal sequence to *ca.* 350 000 years ago using uranium series, which correlates all five with stages 1, 5, 7, 9 and 11, confirming Freyberg's (1973) suggestion that the third sequence is Palaeotyrrhenian. Their elevations thus indicate an uplift rate of *ca.* 0.2 mm a^{-1} (table 3). Vita-Finzi & King (1985) radiocarbon dated this third sequence instead at *ca.* 30 000 years. Although they claimed this as a valid date, it evidently instead marks the age limit of the technique.

Four palaeo-cliffs are identified between these coastal sequences. The base of cliff A is at *ca.* 45 m in the uppermost 'Corinth Marl' beneath the stage 11 sequence: it thus formed during stage 12. Assuming an age of *ca.* 480 000 years and an uplift rate of 0.2 mm a^{-1}, a water level at *ca.* −50 m is indicated. The bases of cliffs B and C are at *ca.* 25 and 15 m in the coastal sediment from stage 11. They were thus incised during stage 10, and indicate a lake level of *ca.* −60 m. Cliff D, at 25 m in the stage 9 sediment, matches the 9a event 280 000 years ago. The upper surface of the stage 9 sediment is exposed down to 5 m elevation. The absence of a visible cliff indicates that the lake level during stage 8 was no shallower than −49 m. Likewise, the lack of

an exposed cliff in the stage 7 sediment indicates a lake level no higher than −38 m during stage 6.

Holocene uplift is indicated by the diolkos, a ramp built around 500 B.C. to allow ships to be dragged across the Corinth isthmus (I3 in figures 2 and 3) (Vita-Finzi & King 1985, figure 16). Holocene beachrock covering it is 0.5 m above present-day high water, indicating uplift at 0.2 mm a^{-1}. Evidence from Kenchriai indicates instead that the Saronic Gulf coast of the isthmus is subsiding at 0.8 mm a^{-1} (table 2). This locality (Vita-Finzi 1986, fig. 98*b*) is in the hanging-walls of the nearby Kechriai and Almiri normal faults (figure 2).

Although most of the Corinth Marl is lacustrine, its top *ca.* 15 m indicates a marine incursion (Collier & Dart 1991), probably around the stage 25 marine highstand *ca.* 900 000 years ago. The canal cut is up to *ca.* 90 m deep, with this marine marl exposed at its highest part; the highest lacustrine marl is at *ca.* 75 m. The oldest marine terrace north of the isthmus is at up to 155 m (Collier & Dart 1991) (I1 in figures 2 and 3), *ca.* 80 m above the youngest lacustrine marl in the isthmus. It is dated to OIT stage 25 given the uplift rates of the younger shorelines nearby (table 3). At the start of the marine highstand around 900 000 years ago this isthmus thus became submerged by *ca.* 80 m. During marine lowstands around this time it presumably maintained PGCB lake level, which was thus *ca.* −80 m. The same terrace is found at 140 m near Loutraki (I2), above a 40 m terrace (Collier & Dart 1991) that is Palaeotyrrhenian if the local uplift rate has been uniform.

Restoring uplift at 0.2 mm a^{-1} places the uppermost Corinth Marl in the isthmus at −2 m during OIT stage 11 around 460 000 years ago. Allowing for margins of uncertainty, it is thus unclear whether a marine connection existed here at this time. However, the top *ca.* 15 m of Corinth Marl, above the first marine incursion, has quite complex structure, with two erosional discontinuities and several other abrupt changes in sedimentary character identified by Collier (1990). These are presumably the remnants of the sediment that was deposited in the marine incursions that did occur between OIT stages 25 and 13.

(ii) *Localities G and S: Alepochori and Megara*

The *ca.* 20 km long, *ca.* 5 km wide and *ca.* 1 km deep Megara Plio-Pleistocene extensional basin is now uplifting and eroding (Bentham *et al.* 1991). At Alepochori, at its NW end and the eastern end of the Alkyonides Gulf (figure 3), the coast (from G1 to G2) is in the footwall of a normal fault, which I call the Alepochori fault. Inland, east of Psatha, this fault offsets a Pleistocene alluvial fan from 550 m to 380 m elevation (Roberts *et al.* 1993). It continues west to the eastern end of the Skinos and Pisia faults that slipped in the February 1981 earthquakes (Jackson *et al.* 1982). Uplifted Pleistocene sediment in its footwall is preserved to *ca.* 350 m elevation *ca.* 6 km SE of Alepochori. Farther southeast, this sediment is gently back-tilted, reaching near sea-level at Megara at the SE end of the basin (Leeder *et al.* 1991). The upper sediment surface projects to *ca.* 600 m at Alepochori, where erosion has reduced elevation to near sea-level. Leeder *et al.* (1991) estimated the erosion from this *ca.* 30 km^2 locality as *ca.* 9 km^3 since *ca.* 1 million years ago, equivalent to a spatial average and time-averaged erosion rate of *ca.* 0.3 mm a^{-1}. This is sufficient to cover the *ca.* 50 km^2 Alkyonides Gulf abyssal plain with *ca.* 180 m thickness of sediment. Seismic reflection profiling indicates that roughly this thickness of sediment is present (Roberts & Stewart 1994), consistent with no local sedimentation having occurred beforehand.

PHILOSOPHICAL TRANSACTIONS OF THE ROYAL SOCIETY A MATHEMATICAL, PHYSICAL & ENGINEERING SCIENCES

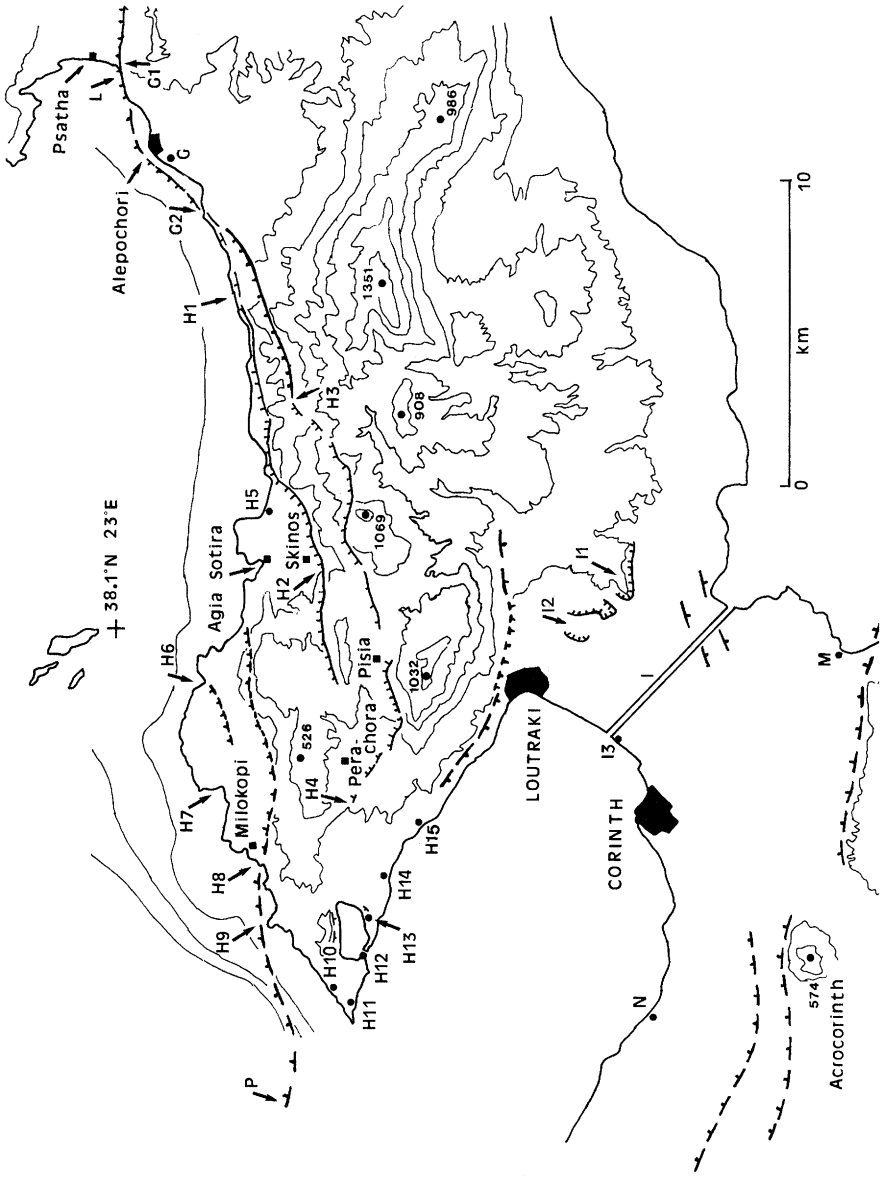

Figure 3. Map of the Perachora peninsula and the northern part of the Corinth isthmus, showing localities G, H, I, L, M, N, and P from the text. Detail southwest of the Corinth canal is omitted (see figure 2). Significant normal faults are shown with hanging-wall ticks; the symbol follows the base of the footwall escarpment. Faulting in the Milokopi area is shown greatly simplified (see text): most fault maps also show an active offshore normal fault continuing ENE to the vicinity of locality H7 (Jackson *et al.* 1982).

During much of early Pleistocene time, the Megara basin was drained axially by a river (Bentham *et al.* 1991). The absolute elevation of the Earth's surface was thus presumably near the lake level in the PGCB, estimated as −80 m. Leeder *et al.* (1991) suggested that upift of this basin interior began around 1 million years ago. The basin surface near Alepochori has thus subsequently uplifted at a time-average rate of *ca.* 0.8 mm a^{-1} (table 3). The basement that is now beneath the Alkyonides Gulf is *ca.* 550 m below sea-level (*ca.* 370 m water depth plus *ca.* 180 m sediment thickness), but was evidently above the level of the PGCB before 1 million years ago, indicating more than 470 m of absolute subsidence or more than 1000 m of subsidence relative to the adjacent interior of the Megara basin at a time-averaged rate of more than

1 mm a^{-1}. Farther east where erosion of material and its resedimentation have been much less important, the 170 m of vertical slip on the Alepochori fault indicates a much lower rate of vertical motion, at less than *ca.* 0.2 mm a^{-1}.

The coast at Alepochori has terraces at 2, 13 and 35 m, which Collier *et al.* (1992) called M1–M3. A 127 000 ± 6 000 year uranium series date of coral from terrace M3 indicates stage 5e, and hence an uplift rate of *ca.* 0.3 mm a^{-1}. Terrace M2, which is not dated, matches stage 5c with the same uplift rate (table 3). The 2 m terrace M1, and nearby 2 m limestone notches in the Alepochori fault footwall at Psatha (L) and Alepochori (G2) (tables 2 and 3), are also not dated. Explaining their 2 m elevation by the sea-level fall over the past 7000 years or so means a zero uplift rate during Holocene time, suggesting that the Alepochori fault ceased to be active beforehand. This fault is south of the south-dipping Kaparelli normal fault, which slipped in the earthquake ($M_s = 6.4$) of 4 March 1981 (Jackson *et al.* 1982).

This Kaparelli fault has slipped only *ca.* 4 m in total, apparently in no more than five earthquakes comparable to this March 1981 event (Roberts *et al.* 1993). Uranium series dating of fault gouge indicates that this fault became active more than 350 000 years ago (Roberts *et al.* 1993), suggesting that at least one of these earthquakes occurred then. The others may have occurred during Holocene time, after slip on the Alepochori fault is inferred to have ceased.

Near Megara (locality S), shorelines at *ca.* 2–3, *ca.* 8–10, and *ca.* 18–20 m (Schröder 1970) match stages 1, 5 and 7 with a *ca.* 0.1 mm a^{-1} uplift rate (table 3). Higher shorelines are too fragmented to be useful. The *ca.* 2–3 m shoreline is documented at many localities between Megara and the Corinth isthmus (Schröder 1970).

Localities P, Q and R: west of the Perachora peninsula Seismic reflection profiles constrain the offshore normal faults west of the Perachora peninsula. Profile P of Brooks & Ferentinos (1984) reveals the sea-floor deepening gently northward to a single major normal fault (P1), where the bathymetry increases from 300 to 800 m with 600 m thickness of tubidites in its hanging-wall. The nearby profile Q of Myrianthis (1984) instead crosses two major normal faults that are *ca.* 2.5 km apart parallel to the ship track. The bathymetry increases across the first (Q1) from 300 to 600 m, then to *ca.* 800 m across the second (Q2). Profile R of Brooks & Ferentinos (1984) shows a single major normal fault across which the bathymetry exceeds 800 m within 3 km of the coast (R1). Figure 2 shows my preferred interpretation, with locality Q at an overlap between normal fault segments where normal faulting steps to the left. If extrapolated onto the Perachora peninsula, the eastern fault coincides with the Milokopi fault identified by Jackson *et al.* (1982).

(iii) *Locality H: The Perachora peninsula*

The north coast of the Perachora peninsula is dominated by a *ca.* 1000 m high north-facing escarpment that contains two main en echelon normal faults (Jackson *et al.* 1982) which slipped in the February 1981 earthquakes ($M_s = 6.7$ and 6.4). I call the northern of these the Skinos fault and the southern the Pisia fault (figure 3). The Pisia fault comprises two main strands *ca.* 100 m apart, with an overall throw of *ca.* 300 m (Roberts *et al.* 1993). The northern of these strands is active, having formed a 130 m high escarpment from which fault gouge has yielded a uranium series date of more than 350 000 years (Roberts *et al.* 1993). The upper bound to the vertical slip rate on this fault is thus *ca.* 0.37 mm a^{-1} (130 m per 350 000 years) (Roberts *et al.* 1993). For comparison, if this normal fault is assumed to have become active

PHILOSOPHICAL TRANSACTIONS OF THE ROYAL SOCIETY A MATHEMATICAL, PHYSICAL & ENGINEERING SCIENCES

Table 3. *Interpretations of palaeoshorelines around the eastern Gulf of Corinth*

(Here and in subsequent tables, stage denotes the OIT stage of formation, from table 1. H in the stage column designates features that post-date the early Holocene marine highstand, and F/S designates normal fault scarps, whose vertical slip rates, U_f, are estimated from variations in uplift rate. Other features are terraces, labelled L if lacustrine. In the header, H and t are the altitude and age of each feature, Z is its uplift, $H - D$, and U is its uplift rate, (H-D)/t, where D is the water level at the time of formation. $\langle U \rangle$ is the average uplift rate of all terraces in a locality (excluding those in parentheses). Uplift rates in square brackets are assumed, in order to estimate water level. Predicted elevations of some missing terraces are also given. The most confidently interpreted features are labelled (*). Data are from Schröder (1970), Leeder *et al.* (1991) and Collier *et al.* (1992) (G and S); Mitzopoulos (1933), Schröder (1970, 1975), Fink & Schröder (1971), Herforth & Richter (1979) (H+R), Richter *et al.* (1979), Vita-Finzi & King (1985), Pirazzoli *et al.* (1994) (H), and Collier (1990), Collier & Dart (1991) and Collier *et al.* (1992) (I, I1 and I2). U, $\langle U \rangle$ and U_f are in mm a^{-1}.)

st.	feature	H/m	t/ka	D/m	Z/m	U	$\langle U \rangle$	U_f
				Locality G: Alepochori				
(1	(*)notch M1	2	7	+1.5–+2	0–0.5	0–0.07)		
5c	(*)notch M2	13	100	−15	28	0.28		
5e	(*)notch M3	35	125	+3	32	0.26	0.27 ± 0.01	
(26L	ELS	600	900	−80	680	0.76)		
				Localities H5 and H6: northern Perachora peninsula (Skinos)				
1	shoreline	2–3	7	+1.5	0.5–1.5	0.07–0.21		
5e	shoreline	8–10	125	+3	5–7	0.04–0.06		
7	shoreline	18–20	250	−5	23–25	0.09–0.10	0.08 ± 0.02	
				Locality H8: Milokopi				
(H	S 92PE8	3.0	5.1	*ca.* 1.0	2.0	0.39)		
(1	(*)notch	3.5 ± 0.2	7	1.5	2.0	0.29)		
				Localities H10 and H11: tip of Perachora peninsula (Heraion)				
(H	HN 2	1.7 ± 0.2	*ca.* 4	*ca.* 0	1.7	0.43±0.05)		
(H	(*)S 92PE5	2.2	4.4	*ca.* 0.5	1.7	0.39)		
(H	(*)S 92PE3	3.1	6.4	1.5	1.6	0.25)		
(1	HN 4	3.2±0.2	7	1.5	1.7	0.24)		
5a	HN 1	1.1±0.2	80	−15	16	0.20		
5c	HN 3	2.6±0.2	100	−15	18	0.18		
5e	(*)terrace	28–30	125	+3	25–27	0.20–0.22		
7a	AB	10–20	200	−25	35–45	0.18–0.23		
7e	terrace	40	250	−5	45	0.18	0.20±0.02	

ELS, elevation limit of sediment; RS, regressional sediment; TS, transgressional sediment; HN, Heraion notch; AB, Algal bioherm; S, sample.

around 0.9 million years ago when sedimentation in the Alkyonides Gulf began, its time-averaged vertical slip rate has been *ca.* 0.33 mm a^{-1} (300 m per 900 000 years). The Skinos fault also has *ca.* 300 m of throw and is assumed to have maintained the same time-averaged slip rate. The south coast of the peninsula is dominated by

Table 3. *Cont.*

stage	feature	H/m	t/ka	D/m	Z/m	U	$\langle U \rangle$	U_f
			Localities H12 and H13: Vouliagmeni					
(H	canal cut	1.7	*ca.* 3	0	1.7	*ca.* 0.57)		
(H	RS	2.0	*ca.* 4	0	2.0	*ca.* 0.50)		
(1	TS	4.0	*ca.* 7	2	2.0	*ca.* 0.29)		
5e	terrace	25	125	3	22	0.18		
7e	HRT-A	40	250	−5	45	0.18	0.18	
F/S	fault	40				—	—	0.12
7e	HRT-B	70	250	−5	75	0.30		
F/S	fault	40				—	—	0.12
7e	HRT-C	100	250	−5	105	0.42		
	terrace	140	360	0	140	0.39	0.40±0.02	
			Localities I and I1: Western part of Corinth isthmus					
H	(*)Diolkos	0.5	2.5	0	0.5	0.20		
5e	(*)ELS	25	125	+3	22	0.18		
(6L	lack of cliff	<0	190	< −38	38	[0.20])		
7e	(*)ELS	45	250	−5	50	0.20		
(8L	lack of cliff	<5	270	< −49	49–54	[0.18–0.20])		
9a	(*)cliff D	25	280	−25	50	0.18		
9e	(*)ELS	75	360	0	75	0.21		
(10L-2	(*)cliff C	15	380	−61	76	[0.20])		
(10L-1	(*)cliff B	25	430	−61	86	[0.20])		
11	(*)ELS	90	460	0	90	0.20		
(12L	(*)cliff A	45	480	−51	91	[0.20])		
25	(*)terrace	155	900	0	155	0.17	0.19±0.02	
(26L	ELS	75	>900	−80	155	0.17)		
			Locality I2: Loutraki					
7e	(*)terrace	40	250	−5	45	0.18		
25	(*)terrace	140	900	0	140	0.16	0.17±0.01	
			Locality S: Megara					
(1	shoreline	*ca.* 2–3	7	+1.5–+2	0.5–1.5	0.07–0.21)		
5e	shoreline	*ca.* 10	125	+3	7	0.06		
7e	shoreline	*ca.* 20	250	−5	25	0.10		
26L	ELS	*ca.* 0	900	*ca.* −80	80	0.09	0.09	

ELS, elevation limit of sediment; RS, regressional sediment; TS, transgressional sediment; HRT-A,-B,-C, Herforth & Richter (1979) terrace A,B,C.

another *ca.* 1000 m high escarpment, inland of Loutraki, which exposes the footwall of a south-dipping normal fault. The Pliocene Corinth basin and the modern Corinth isthmus are both situated in the hanging wall of this fault (Collier & Dart 1991).

South of its western end, the *ca.* 200 m deep Lecheon Gulf is underlain by *ca.* 500 m of Pliocene and younger sediment, such that the estimated vertical slip on this Loutraki normal fault is *ca.* 1700 m.

The Skinos fault slipped in 1981 between localities H1 and H2 (figure 3), and the Pisia fault slipped between H3 and H4. Up to 1.5 m overall vertical slip across both faults is indicated, with slip on the Skinos fault greatest east of Strava (H5) near the eastern end of the slip on the Pisia fault. Other apparently active normal faults cut across this peninsula, for instance near Milokopi (H8), but did not slip in 1981. Because both earthquakes occurred during the same night (24–25 February 1981), it was initially unclear which caused the observed fault scarps.

The Skinos fault hanging-wall subsided in 1981, as is evident from the inundated chapel at Strava (H5) (Vita-Finzi 1986, fig. 98*a*) and geodetic observations (Stiros 1986). Jackson *et al.* (1982) deduced longer-term subsidence between H1 and H6 from the marshy coastline. However, shorelines and wavecut platforms at *ca.* 2–3, *ca.* 8–10 and *ca.* 18–20 m between sites H5 and H6 (Schröder 1970) indicate longer-term uplift instead, at a rate of *ca.* 0.1 mm a^{-1} (table 3). Jackson *et al.* (1982) accepted this evidence of uplift (raised beaches and limestone notches) west of H7 (see Vita-Finzi & King (1985, fig. 9)), which they interpreted as footwall uplift from an offshore normal fault. They suggested that the 1981 mainshock occurred on this fault, uplifting this coastline, and the second event caused all the faulting on the peninsula. Many people questioned this interpretation. For instance, Carydis *et al.* (1982) suggested that the Perachora fault scarps were caused by both events. Westaway & Smith (1989) noted that the seismic moment of the second earthquake was far too small to account for all the surface faulting: at least some of it was produced by the mainshock. Taymaz *et al.* (1991) finally retracted the Jackson *et al.* (1982) interpretation. The 1981 mainshock presumably caused the longer Pisia fault scarp that persists farther west, the Skinos scarp being produced by the second event (figure 3).

Schröder (1970), Herforth & Richter (1979) and Richter *et al.* (1979) described marine terraces at up to *ca.* 140 m at sites H10–H13 near the tip of the peninsula. The most reliable evidence for long term uplift is the 28 m shoreline at locality H10 inferred as Eutyrrhenian from the presence of *Strombus bubonius* (Mitzopoulos 1933), indicating an uplift rate of *ca.* 0.2 mm a^{-1}. Bioherms identified at locality H10 at 10–20 m elevation by Richter *et al.* (1979) in a position that is stratigraphically beneath the Eutyrrhenian shoreline are interpreted here as from the 7a event *ca.* 200 000 years ago. The fossil assemblage indicates that the Gulf was brackish when these bioherms were formed (Richter *et al.* 1979), indicating only a limited connection with the open sea.

Vita-Finzi & King (1985, fig. 17) also documented site H10 north of Cape Heraion, and Pirazzoli *et al.* (1994) described in detail the adjacent locality H11 near the ancient Heraion temple. These localities and the nearby Vouliagmeni lagoon (H12–H13) have proved particularly controversial. Pirazzoli *et al.* (1994) showed using before and after photographs that this coastline did not change measurably during the 1981 earthquakes: it neither uplifted as Jackson *et al.* (1982) claimed, nor subsided as Vita-Finzi & King (1985) claimed. Pirazzoli *et al.* (1994) also dismissed several archaeological features that some previous studies had used to infer longer-term subsidence in this area. Several studies have also noted notches in the limestone coast near modern sea-level. Pirazzoli *et al.* (1994) measured their altitudes as 3.2, 2.6, 1.7, and 1.1 m, all ±0.2 m. Samples of *Lithophaga* (rock-boring molluscs), whose upper altitude limit is a sensitive indicator of sea-level, were radiocarbon dated to

PHILOSOPHICAL TRANSACTIONS OF THE ROYAL SOCIETY A MATHEMATICAL, PHYSICAL & ENGINEERING SCIENCES

6400 years (3.1 m altitude) and 4400 years (2.2 m altitude) (Pirazzoli *et al.* 1994). Furthermore, a canal was dug between the Vouliagmeni lagoon and the sea during antiquity (say *ca.* 3000 years ago), and was reopened by a new excavation in the late 19th century (Vita-Finzi & King 1985). Vita-Finzi & King (1985) found *Notirus irus*, which lives in the intertidal range, at 1.7 m elevation along its cut, indicating at least this amount of uplift since the canal was dug. As already noted, their *ca.* 7000 year dates for these samples are not archaeologically feasible. Fink & Schröder (1971) described marine sediment marking an early Holocene transgression to *ca.* 4 m above present day sea-level around this canal cut, partly overlain (below *ca.* 2 m altitude) by a regressional sequence containing debris that is archaeologically dated to *ca.* 2000–1600 B.C. Pirazzoli *et al.* (1994) regarded all four notches as Holocene, interpreting them as evidence of repeated offshore earthquakes each causing *ca.* 0.8 m of uplift. As they noted, this requires much higher uplift rates than the Late Pleistocene evidence. Table 3 suggests an alternative interpretation in which notches 3 and 1 are regarded as from stages 5c and 5a, with uplift rates consistent with the older evidence. Notches 4 and 2 are thus interpreted as marking the early Holocene marine highstand about 7000 years ago and the stable sea-level over the past 4000 years or so. The evidence that all features younger than *ca.* 7000 years at localities H10 to H12 have uplifted *ca.* 1.7 m points to one very large Late Holocene offshore earthquake. The ratio of its *ca.* 1.7 m of uplift to the *ca.* 0.2 mm a^{-1} long-term uplift rate implies recurrence every *ca.* 9000 years, so only one such event is indeed expected during the Holocene. The late Pleistocene uplift rates average out the effects of many earthquake cycles. This point is important, because if the interpretation by Pirazzoli *et al.* (1994) were correct, then any relative dating scheme (such as that proposed by Keraudren & Sorel (1987)) which assumes roughly uniform uplift rates for the Pleistocene palaeoshorelines elsewhere in the Gulf would be undermined.

At Milokopi (locality H8), a tombolo has a notched shoreline with the highest notch at +3.5 m, and a specimen of *Lithophaga* from 3.0 m above its living counterparts has been radiocarbon dated to *ca.* 5000–5200 years (Pirazzoli *et al.* 1994). These data are consistent with 2 m of uplift in a single late Holocene offshore earthquake, rather than 1.7 m as at localities H10–H12, suggesting closer proximity to the offshore fault that slipped. Figure 3 greatly simplifies the observed faulting in this area: warping of palaeoshorelines both north and south of Milokopi (Vita-Finzi & King 1985; Pirazzoli *et al.* 1994) reveals several minor normal faults that intersect the coastline.

Finally, Herforth & Richter (1979) reported marine terrace fragments at locality H13 at 40, 70, 100, and 140 m elevations. They showed that the three lowest all have the same degree of diagenesis, which matches that of the Palaeotyrrhenian deposits in the Corinth canal cut. These observations support an eastward increase in uplift rate from *ca.* 0.1 to *ca.* 0.4 mm a^{-1} (table 3) in *ca.* 500 m distance, caused either by active faulting or by westward tilting. Such an increase in uplift rate is required to match the uplift rates required in the footwalls of the major active normal faults farther east along the Perachora peninsula (figure 3).

(iv) *Locality A1: Corinth to Xylokeriza*

Keraudren & Sorel (1987) noted terraces at 15 m (5.1), 30 m (New Corinth, or 5.5), 45 m (Tripos, or 7.1), 65 m (Ancient Corinth, or 7.3), and 80 m (Temple, or 7.5). Collier *et al.* (1992) estimated their elevations instead as 14, 28, 46, 64 and 80 m. The New Corinth terrace at site A1A is documented by Vita-Finzi & King (1985, fig. 20). Collier *et al.* (1992) published uranium series dates from site A1B, in the lower part

PHILOSOPHICAL TRANSACTIONS OF THE ROYAL SOCIETY A MATHEMATICAL, PHYSICAL & ENGINEERING SCIENCES

of the Ancient Corinth (7.3) terrace. The dates of 177 000+11 000/−10 000 years and 232 000 + 24 000/ − 20 000 years average to *ca.* 205 000 years, so this terrace formed following the 7c event. It is thus correctly identified by Keraudren & Sorel (1987), along with the neighbouring Tripos, New Corinth, and Temple terraces, which all indicate an uplift rate of *ca.* 0.3 mm a^{-1} (table 3). The New Corinth terrace is thus Eutyrrhenian, as is expected from its *Strombus bubonius* fauna; the *ca.* 30 000 year radiocarbon date by Vita-Finzi & King (1985) is presumably another lower bound to age that is limited by the method.

(v) *Locality A2: Lecheon to Penteskoufi*

Cross-section A2 passes 4 km west of Akrocorinth, where basement has uplifted in the footwall of a north-dipping normal fault that I call the Akrocorinth fault (figures 2–3). With the Ancient Corinth and Temple terraces correlated as before, their uplift rate is *ca.* 0.4 mm a^{-1} (table 4). If the highest terraces also correlate as suggested by Keraudren & Sorel (1987), their uplift rate is *ca.* 0.6 mm a^{-1}. However, there is now no separate marine highstand with which to correlate their 8.1 terrace. This also cannot be the lacustrine terrace from stage 8, as *ca.* 45 m of uplift (from *ca.* −50 m to more than −5 m) is needed between 270 000 and 250 000 years ago for this to remain exposed above the stage 7e terrace, requiring an uplift rate above 2 mm a^{-1}. This terrace is roughly in line with the Akrocorinth fault and a north-dipping normal fault that Keraudren & Sorel (1987) identified farther west (figure 2), and is interpreted as the stage 7e terrace repeated in the footwall of this fault. This footwall has evidently uplifted at *ca.* 0.6 mm a^{-1}, indicating a vertical slip rate of *ca.* 0.2 mm a^{-1}. However, the terraces close to this fault show intermediate uplift rates, suggesting that part of this vertical slip is distributed over a substantial zone, rather being localized on a single fault strand.

The absence of terraces younger than Palaeotyrrhenian (Tripos/7.1) indicates very slow uplift of the present-day coast around Lecheon. The *ca.* 2000 year old port of Lechaeum has indeed subsided 0.7 m according to Flemming (1978) (table 2). This absence of uplift can be explained by a component of hanging-wall subsidence beside a normal fault north of the Tripos (7.1) terrace. Significant active normal faulting in this locality is expected, because it was the epicentral area of the destructive ($M_s \approx 7$) earthquake of 21 February 1858 (Comninakis & Papazachos 1982). By analogy with the Perachora peninsula, it is unlikely that the subsidence over 2000 years is representative of long term. My preferred interpretation in table 4 thus regards this terrace sequence as faulted twice. I designate as the Lecheon fault the normal fault north of the Tripos terrace, and estimate its probable long-term vertical slip rate as *ca.* 0.3 mm a^{-1}.

(vi) *Locality B: Velon to west of Stimanga*

Locality B is more than 10 km WNW of A2 and 4 km ESE of the Kiaton-Souli section (table 4). Each terrace is again interpreted consistent with Keraudren & Sorel (1987), with terrace 8.1 again regarded as a repeat of terrace 7.5 in the footwall of an active normal fault. Terraces above 8.1 are uplifting at *ca.* 0.8–0.9 mm a^{-1}, whereas those below are uplifting at *ca.* 0.6-0.7 mm a^{-1}, again indicating that a normal fault with a vertical slip rate of *ca.* 0.2 mm a^{-1} is present. The lowest terrace (5.5; New Corinth) has an uplift rate of only *ca.* 0.4 mm a^{-1}. A second fault is thus required between it and the Ancient Corinth terrace, with a vertical slip rate of *ca.* 0.3 mm a^{-1}. The lake level during stage 8 is thus estimated as −50 m, consistent with the previous

PHILOSOPHICAL TRANSACTIONS OF THE ROYAL SOCIETY A MATHEMATICAL, PHYSICAL & ENGINEERING SCIENCES

estimates. I tentatively suggest that the faults offsetting these terraces are equivalent to faults F11 and F10 of Doutsos & Piper (1990) at Kiaton farther west (see below), and the Lecheon and Akrocorinth faults to the east.

(vii) *Locality C: Xylokastron*

The final Keraudren & Sorel (1987) terrace locality is 14 km WNW of Velon (table 4) (see also Doutsos & Piper 1990, fig. 8*a*). Keraudren & Sorel (1987) noted terrace multiplets around the 5.1 and 5.5 highstands west of Pasia (figure 2). Similar multiplets are documented in other rapidly uplifting localities on sheltered coastlines (Westaway 1993*b*), and reflect short-term sea-level changes around highstands. This coast is in the footwall of a major offhore normal fault zone 2–3 km offshore, whose hanging-wall is beneath the abyssal plain deeper than 800 m where sediment is *ca.* 1 km thick (Brooks & Ferentinos 1984). The cross-section drawn by Leeder & Jackson (1993, fig. 8*b*) along Brooks & Ferentinos's (1984) seismic profile (R in figure 2) instead shows a maximum of almost 500 m of water underlain by *ca.* 500 m of sediment, and evidently underestimates the true vertical scale by a factor of two. There is no evidence of any onshore normal fault at Xylokastron (Leeder & Jackson 1993).

Terraces 3.1, 3.3 and 5.1 unambiguously match stages 3a, 3c and 5a with an uplift rate of *ca.* 1.5–1.6 mm a^{-1}; wildly discrepant uplift rates are otherwise obtained. Keraudren & Sorel's (1987) correlation of the 5.5 terrace multiplet with the New Corinth (stage 5e) terrace farther east, with an uplift rate of *ca.* 1.4 mm a^{-1} and with terrace 5.3 assigned to stage 5c, is also unequivocal. However, they were uncertain about how the highest terraces at Xylokastron correlate with localites farther east, from which they are isolated by a *ca.* 3 km wide zone of erosion (figure 3). They included one terrace (labelled ?, which I call 6.1 to fit their scheme), which they could not explain, and another (6.3), which they interpreted as a marine terrace from the stage 6 glacial maximum. If their terrace 6.3 is correlated instead with the 7a highstand, an uplift rate of 1.6 mm a^{-1} is required. Scarp 6.1 may thus indicate a normal fault with a vertical slip rate of *ca.* 0.2 mm a^{-1}. However, terrace 6.5 would now not match any known marine highstand. A second interpretation would assign terrace 6.5 to the 7a event, and the oldest terrace (7.5) to 9a, with an uplift rate of *ca.* 1.5 mm a^{-1} for the oldest part of the sequence. Terraces 6.1 and 6.3 both now match no known marine highstand.

My preferred interpretation (table 4) instead assigns terrace 6.3 to the 7a event, and the oldest terrace (7.5) to 9c. Scarp 6.1 cannot now be a normal fault scarp because the required vertical slip rate is zero. It is interpreted instead as a lacustrine terrace from stage 6, with the water level at −40 m. This terrace sequence is thus not faulted, as is expected. The uplift rate variation from *ca.* 1.6 to 1.2 mm a^{-1} over *ca.* 2 km distance indicates back-tilting at (0.4 mm a^{-1}/2 km) × 180°/π or *ca.* 11° Ma^{-1} behind the offshore normal fault. The Keraudren & Sorel (1987) correlation thus breaks down for the oldest part of this terrace sequence. For instance, the terrace that they labelled 7.5 dates from the 7e event (250 ka) elsewhere.

(viii) *Locality E: Derveni*

At Derveni, 20 km WNW of Xylokastron, a series of uplifted fan-deltas and foreset and bottomset sequences overlies three major WNW-striking normal faults that bound the south coast of the Gulf (figure 4) (Ori 1989; Doutsos & Piper 1990, fig. 5g). A fourth fault farther inland south of Karia bounds the PGCB, with the 2376 m

PHILOSOPHICAL TRANSACTIONS OF THE ROYAL SOCIETY A MATHEMATICAL, PHYSICAL & ENGINEERING SCIENCES

Table 4. *Interpretations of terraces inland of Corinth, Lecheon, Velon, and Xylokastron*

(Data are from Keraudren & Sorel (1987) (K&S) and Flemming (1978) (A2), and Keraudren & Sorel (1987) (A1, B and C). See table 3 caption for notation. The Agios Spiridon terrace at locality A1 could also match stage 5a with an uplift rate of 0.38 mm a^{-1}. U, $\langle U \rangle$ and U_f are all in mm a^{-1}.)

stage	feature	H/m	t/ka	D/m	Z/m	U	$\langle U \rangle$	U_f
	Locality A1: Corinth to Xylokeriza							
5c	(*)Agios Spiridon terrace (5.1)	15	100	−15	30	0.30		
5e	(*)New Corinth terrace (5.5)	30	125	+3	27	0.22		
(6L	obliterated by terrace 5.5	17	190	−40	57	[0.30])		
7a	(*)Tripos terrace (7.1)	45	200	−25	70	0.35		
7c	(*)Ancient Corinth terrace (7.3)	65	230	−5	70	0.30		
7e	(*)Temple terrace (7.5)	80	250	−5	85	0.34	0.34±0.03	
(8L	obliterated by terrace 7.5	45	270	−50	95	[0.35])		
	Locality A2: Lecheon to Penteskoufi							
(H	(*)Lechaeum harbour	−0.7	2.0	0	−0.7	−0.35	−0.35)	
F/S	Lecheon fault	*ca.* 60						(0.7)
7c	(*)Ancient Corinth terrace (7.3)	75	230	−5	80	0.35		
7e	(*)Temple terrace (7.5)	100	250	−5	105	0.42	0.39±0.03	
F/S	Akrocorinth fault	< 115						0.2
7e	K&S terrace 8.1	115	250	−5	120	0.48		
(8L	obliterated by terrace 8.1	85	270	−50	135	[0.50])		
9a	K&S terrace 8.5	135	300	−30	165	0.55		
9c	K&S terrace 9.1	185	330	−10	195	0.59		
9e	Nicoletto terrace (9.3)	215	360	0	215	0.60		
(10L	obliterated by terrace 9.3	175	400	−65	240	[0.60])		
11	Veliniatika terrace (11.3)	310	460	0	310	0.67	0.61±0.02	
(12L	obliterated by terrace 11.3	240	480	−50	290	[0.60])		
(F/S	Kenchriai fault	*ca.* 300						0.3)

summit of mount Killini in its footwall. The oldest fan delta system (Evrostini) is between faults 2 and 3. Near fault 3, the base of its topsets is now at *ca.* 900 m; their upper surface rises to 1208 m, but is back-tilted SSW by 5°. The base and top of its bottomsets are now at *ca.* 700 and *ca.* 800 m. The Gulf was thus *ca.* 200 m deep when this system became active, and *ca.* 400 m deep when its activity ceased. In the hanging wall of fault 2, the Evrostini topsets span 700–1000 m altitude, overlying the older lacustrine PGCB sediment (Ori 1989). The uppermost PGCB sediments are back-tilted at 10° at Mavron (summit 1757 m), behind fault 2. An estimated 1057 m of vertical slip (1057–700 m) has thus occurred on fault 2 since the end of PGCB sedimentation. The second fan delta system (Ilias) is between faults 3 and 4. Its upper surface is now back-tilted from *ca.* 400 m elevation near the coast to *ca.* 300 m near fault 3. On its seaward face, and at other localities nearby, a marine terrace is visible at *ca.* 200 m. The modern fan delta system is in the hanging-wall of fault 4: its foresets reach offshore with bottomsets on the Gulf abyssal plain.

Table 4. *Cont.*

stage	feature	H/m	t/ka	D/m	Z/m	U	$\langle U \rangle$	U_f
			Locality B: Velon to west of Stimanga					
5e	New Corinth terrace (5.5)	55	125	+3	52	0.42	0.42	
(6L	obliterated by terrace 5.5	36	190	−40	76	[0.40])		
F/S	Fault F11/Lecheon fault	> 55						0.2
7a	Tripos terrace (7.1)	90	200	−25	115	0.58		
7c	(*)Ancient Corinth terrace (7.3)	140	230	−5	145	0.63		
7e	(*)Temple terrace (7.5)	165	250	−5	170	0.68	0.63±0.05	
F/S	Fault F10/Akrocorinth fault	> 165						0.1
7e	K&S terrace 8.1	185	250	−5	190	0.76		
(8L	obliterated by terrace 8.1	166	270	−50	216	[0.80])		
9a	K&S terrace 8.5	215	300	−30	245	0.82		
9c	K&S terrace 9.1	250	330	−10	260	0.79		
9e	Megali Lakka terrace (9.3)	320	360	0	320	0.89	0.82±0.05	
(10L	obliterated by terrace 9.3	300	400	−60	360	[0.90])		
			Locality C: Xylokastron					
(2L	predicted terrace elevation	20	45	−52	72	[1.60])		
3a	K&S terrace 3.1	40	50	−35	75	1.50		
	(*)K&S terrace 3.3	65	60	−30	95	1.58		
5a	(*)Agios Spiridon terrace (5.1.1)	100	*ca.* 80					
	(*)K&S terrace 5.1.3	105	80	−15	120	1.50		
5c	(*)Konoukles terrace (5.3)	120	100	−15	135	1.35		
5e	New Corinth terrace (5.5.1)	150	*ca.* 120					
	K&S terrace 5.5.3	160	*ca.* 120					
	(*)K&S terrace 5.5.5	170	125	+3	167	1.34		
(6L	K&S terrace 6.1	205	190	−42	247	[1.30])		
7a	K&S terrace 6.3	230	200	−25	255	1.28		
7c	K&S terrace 6.5	275	230	−5	280	1.22		
7e	K&S terrace 7.1	310	250	−5	315	1.26		
(8L	obliterated by terrace 7.1	290	270	−50	340	[1.25])		
9a	K&S terrace 7.3	330	300	−30	360	1.20		
9c	K&S terrace 7.5	365	330	−10	375	1.14	1.30±0.10	

Sediment in this locality lacks age indicators (Ori 1989). However, from discussion above it is likely that the oldest fan delta system became active around 900 000 years ago. Assuming that slip on fault 2 began at this time, and the PGCB lake level was −80 m, its footwall has uplifted at a time-averaged rate of *ca.* 1837 m/0.9 Ma or *ca.* 2 mm a^{-1}. The back-tilting rate of the youngest PGCB sediments has thus been *ca.* 10°/0.9 Ma or *ca.* 11° Ma^{-1}. Given the *ca.* 700 m elevation of the top of the PGCB sediment in the hanging-wall of fault 2, the average uplift of its footwall and hanging-wall is thus (1837 + 780)/2 m or *ca.* 1300 m, suggesting a time-averaged local uplift rate of *ca.* 1.4 mm a^{-1} if the effect this fault is excluded. Assuming that deposition

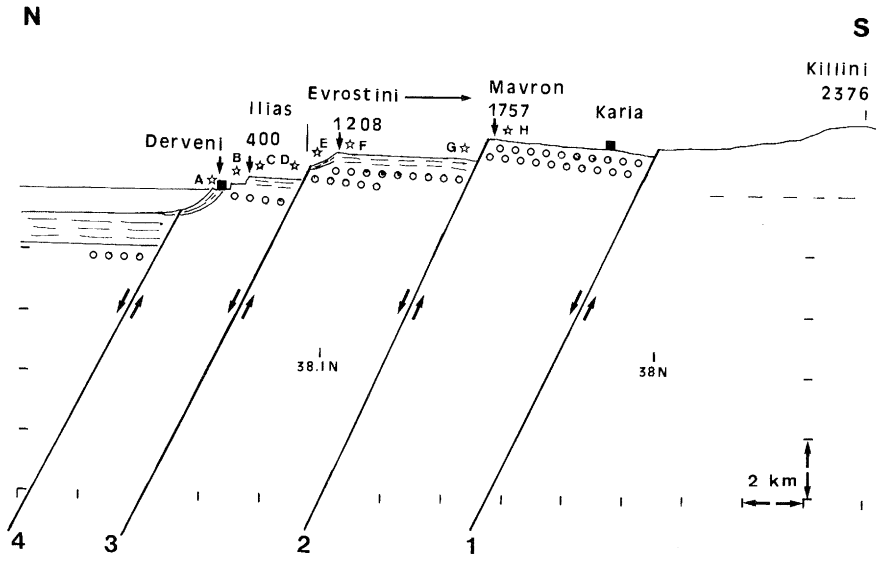

Figure 4. North-south cross-section along longitude 22.4° E through the uplifted south coast of the Gulf of Corinth between Derveni and Killini, showing (with no vertical exaggeration) the tilt and uplift of the Plio-Pleistocene lacustrine PGCB sediment (open circles) and the overlying late Pleistocene deposits (line shading) from the Evrostini, Ilias, and modern fan-delta systems. A denotes the topsets of the modern fan-delta system on which Derveni is built. B denotes the *ca.* 200 m marine terrace that is interpreted as Eutyrrhenian; C-D denotes the topsets of the Ilias fan-delta system, which are at present back-tilted from *ca.* 400 m elevation at C to *ca.* 300 m at D. E denotes the Evrostini foreset and bottomset sequence. The bottomsets span the present-day elevation range 700–800 m. F-G denotes the Evrostini topsets, which are back-tilted at *ca.* 5°. At F, these sediments are found above *ca.* 900 m elevation. H denotes the youngest exposed PGCB sediment at the summit of Mavron. Major normal faults 1–4 are drawn planar with 65° dip to *ca.* 10 km depth. Adapted from Ori (1989, figure 3), which shows more detail of the sedimentary sequences.

of the Evrostini fan delta system ceased when faulting migrated to fault 3 and fault 2 became inactive, and footwall uplift continued at roughly the same rate as before, this system was last active around the 780 000 year (stage 19) marine highstand, when the Ilias system became active. Its surface has thus subsequently tilted at *ca.* 5°/0.78 Ma or *ca.* 6° Ma^{-1}; faster, if allowance is made for any depositional dip. The *ca.* 1057 m of estimated vertical slip across fault 2 thus developed in *ca.* 270 000 years, indicating a vertical slip rate of *ca.* 3.9 mm a^{-1}. Similar reasoning suggests that the Ilias system was active until the stage 7 highstand. The subsequent uplift rate of its *ca.* 2 km wide surface varies from 1.6 mm a^{-1} near the coast to *ca.* 1.2 mm a^{-1} near fault 3, indicating a tilt rate of *ca.* (0.4 mm a^{-1}/2 km) × 180°/π or *ca.* 11° Ma^{-1}. With an uplift rate of *ca.* 1.5 mm a^{-1}, the 200 m marine terrace correlates with OIT stage 5e.

(ix) *Locality U: Kamari to Pellini*

Kamari is 14 km ESE of Derveni and 6 km WNW of Xylokastron. About 2 km inland the land surface rises abruptly to a flat summit at 732 m, on an escarpment that is an inline continuation of the footwall of fault 3 at Derveni. Farther inland, the Earth's surface elevation drops to *ca.* 420 m for *ca.* 1 km, then rises to *ca.* 460 m for *ca.* 2 km, before rising again to another flat summit at 804 m, capped by PGCB

Table 5. *Interpretations of terrace sequences inland of Derveni and Kiaton*

(Data from Ori (1989) (E), and Sauvage & Dufaure (1976), Sébrier (1977), Vita-Finzi & King (1985), Keraudren & Sorel (1987), and Doutsos & Piper (1990) (D). Codes F8–F12 for normal faults and A, B, C1, C2, and D for terraces are from Doutsos & Piper (1990). U, $\langle U \rangle$ and U_f are all in mm a^{-1}.)

stage	feature	H/m	t/ka	D/m	Z/m	U	$\langle U \rangle$	U_f
			Locality E: Derveni					
5e	terrace	200	125	+3	197	1.58		
7e	top Ilias topset	400	250	−5	405	1.62		
17	(*)top Evrostini topset	1208	780	−10	1218	1.56	1.59±0.03	
(25	(*)base Evrostini topset	900	900	0	900	1.00)		
(26L	(*)Mavron	1757	$\gtrsim$900	−80	1837	2.04)		
			Locality T: Kamari to Pellini					
15	terrace	732	620	−10	742	1.20		
9e	terrace	420	360	0	420	1.17		
11	terrace	460	460	0	460	1.00		
26L	terrace	804	>900	−80	884	0.98	1.09±0.10	
			Locality D: Kiaton to Souli					
5e	New Corinth terrace	50	125	+3	47	0.38		
F/S	fault F12	50						0.1
5e	New Corinth terrace (5.5/D)	60	125	+3	57	0.46		
(6L	River terrace	80–60	190	−8–−28	88	[0.46])		
F/S	fault F11	>80						0.6
7a	Tripos terrace (7.1/C2)	180	200	−25	205	1.03		
F/S	fault F10	240						0.2
7c	ancient Corinth terrace (7.3)	280	230	−5	285	1.24		
7e	Temple terrace (7.5/C1)	300	250	−5	305	1.22		
(8L	obliterated by 7.5	274	270	−50	324	[1.20])		
9a	K&S terrace 8.5	330	300	−30	360	1.20		
9c	K&S terrace 9.1	400	330	−10	410	1.24		
9e	Megali Lakka terrace (9.3/B)	420	360	0	420	1.17	1.21±0.04	
(10L	obliterated by terrace 9.3	407	400	−61	468	[1.17])		
F/S	fault F9	<600						0.1
11	Souli terrace (11.3/A)	620	460	0	620	1.35		
(12L	obliterated by terrace 11.3	598	480	−50	648	[1.35])		
26L	terrace	820	>900	−80	900	1.00		
	fault F8	820						0.1
26L	terrace	940	>900	−80	1020	1.13		

lacustrine sediment (Ori 1989), up a second escarpment that is an inline continuation of the footwall of fault 2 at Derveni. The more subdued form of these escarpments compared with at Derveni suggests that the vertical slip on both normal faults dies

PHILOSOPHICAL TRANSACTIONS OF THE ROYAL SOCIETY A MATHEMATICAL, PHYSICAL & ENGINEERING SCIENCES

Table 6. *Vertical slip rates on active normal faults between Kiaton and Souli*
(Y is the fault offset (from Doutsos & Piper 1990); t is its age; U_y is the vertical slip rate estimated as Y/t; U_f is the vertical slip rate estimated from lateral variations in uplift rate.)

fault	Y/m	t/ka	U_y/(mm a^{-1})	U_f/(mm a^{-1})
F12	10	125	0.08	0.1
F11	>60	200	>0.30	0.6
F10	40	230	0.17	0.2
F9	40	460	0.09	0.1
F8	>50	900	>0.06	0.1

out eastward, consistent with the absence of slip at Xylokastron. The tentative interpretation in table 5 indicates a gradual landward decrease in time-averaged uplift rate from *ca.* 1.2 to *ca.* 1.0 mm a^{-1}, consistent with the active normal faulting now being offshore. A sequence of young marine terraces like at Xylokastron is thus predicted directly inland of Kamari; those nearest the coast are expected to be uplifting at *ca.* 1.5–1.6 mm a^{-1}.

(x) *Locality D: Kiaton to Souli*

The controversial Kiaton to Souli section has been investigated in detail by Sauvage & Dufaure (1976), Vita-Finzi & King (1985), and Doutsos & Piper (1990). Table 5 shows my preferred interpretation, which requires faulted offsets to the terraces below Souli at the four major faults (F9–F12) identified by Doutsos & Piper (1990). From the changes in uplift rate, their vertical slip rates are *ca.* 0.1 (F12), *ca.* 0.6 (F11), *ca.* 0.2 (F10) and *ca.* 0.1 mm a^{-1} (F9). Slip rates from the ages and offsets across these faults confirm these estimates (table 6).

I regard the Souli terrace above 600 m as from OIT stage 11. This terrace has thus uplifted at *ca.* 1.35 mm a^{-1}, one of the fastest uplift rates anywhere around the Gulf, although the uplift near the coast at Kiaton is much slower. The terraces south of Souli, which are in PGCB lacustrine sediment (Doutsos & Piper 1990), are assumed to be older than *ca.* 900 000 years and to be offset by faulting. My interpretation includes the terrace at *ca.* 820 m (Sauvage & Dufaure 1976) near Souli, *ca.* 2 km southwest of the terrace from stage 11. If this is more than *ca.* 900 000 years old, an uplift rate of *ca.* 1 mm a^{-1} is indicated. The resulting *ca.* 0.35 mm a^{-1} decrease in uplift rate in *ca.* 2 km distance southwest of Souli indicates back-tilting at *ca.* 10° Ma^{-1}. Farther southwest, the uplift rate increases again by *ca.* 0.1 mm a^{-1} as a result of the vertical slip on fault F8 (from Doutsos & Piper 1990).

Doutsos & Piper (1990) noted that the scarp of fault F11 also separates a marine terrace above (7.1/Tripos) from a river terrace below. This river terrace slopes seaward from *ca.* 80 to *ca.* 60 m, before being buried beneath the New Corinth (5.5) terrace. I suggest that it formed during OIT stage 6 with its lower limit more than 10 m above lake level.

(xi) *Locality F: Kastraki to Psari*

My final locality is the SW end of Doutsos & Piper's (1990) profile through the PGCB (figure 3). Sediments are locally back-tilted at up to *ca.* 10° by slip on NE-dipping normal faults. The landscape is broken up by three major faults, F1–F3

PHILOSOPHICAL TRANSACTIONS OF THE ROYAL SOCIETY A MATHEMATICAL, PHYSICAL & ENGINEERING SCIENCES

(figure 3). From offsets of basement, Doutsos & Piper (1990) estimated their vertical displacements as 700, 700 and 300 m. F1, with basement in its footwall, marks the PGCB margin. The late Calabrian lacustrine conglomerate is locally well-exposed, and forms most of the topography, including the 1209 m summit of mount Gathrios east of Asprokambos in the footwall of fault F3. The top of this conglomerate is also found at 1000 m at Psari in the footwall of fault F2, at 800 m in its hanging-wall, and at 900 m at Kastraki in the hanging-wall of F3; further northeast it is eroded.

From the offsets to this conglomerate, which marks the end of PGCB sedimentation, *ca.* 200 m of the displacement on fault F2 and all the *ca.* 300 m displacement on F3 are estimated to have developed over the past 0.9 million years, at time-averaged vertical slip rates of *ca.* 0.2 and 0.3 mm a^{-1}. With a uniform vertical slip rate, fault F2 thus formed around 3 million years ago. Fault F1 is evidently older, and is presumed to date from the start of local extension *ca.* 5 million years ago. With the late Calabrian lake level at −80 m, uplift rates of 1.1 and 0.9 mm a^{-1} over the past 0.9 million years are indicated for the footwall and hanging-wall of F2, and 1.3 and 1.0 mm a^{-1} for the footwall and hanging-wall of F3.

4. Summary of observations

Tables 3 to 5 list these elevation change data and their interpretations. Predicted rates of elevation change of modern coastlines range from zero or negative values to 1.6 mm a^{-1} at Xylokastron and Derveni. The interpretation scheme is internally consistent, as except for subsurface exposures (as in the Corinth Canal) and limestone notches, the terraces listed are all expected to be exposed with the interpreted uplift rate. Denis Sorel (personal communication, 1994) has claimed that my interpretation of fault scarps offsetting terraces of different ages is contentious. Most fault scarps follow terrace margins because the difference between the footwall and hanging-wall uplift rates of these faults is sufficient for the hanging-wall to be submerged or to be eroded by the sea during an interglacial marine highstand after the last time when the footwall was submerged. In each case the fault thus briefly bounds the coastline. For instance, at Velon (table 4), after the footwall of the Lecheon fault was last submerged *ca.* 200 000 years ago this fault bounded the coastline during the stage 5e highstand, when the New Corinth terrace formed in its hanging wall. The terrace from 200 000 years ago is predicted at *ca.* 55 m in this hanging wall, the same altitude as the stage 5e terrace, and was thus either bured or eroded during stage 5e. Other faults may well also offset individual terraces, but to avoid this effect their vertical slip rates have to be very low. Such faults may explain some of the lateral variations in uplift rate reported within terrace sequences, but do not contribute significantly to the region's extension and are thus omitted here.

Denis Sorel (personal communication, 1994) also notes several localities where individual terraces contain both marine and lacustrine fauna. These include the New Corinth terrace west of Corinth town (terrace 5.5 near locality A1), terrace 9.3 at locality A2, and terrace 7.3 at locality D. These freshwater components may each be reworked from the preceding lacustrine terrace (6L, 10L, and 8L, respectively).

Figure 5 summarizes my results for elevation change around the Gulf of Corinth during the past *ca.* 0.9 million years. The uplift rate near the south coast of the Gulf increases westward from *ca.* 0.1 mm a^{-1} at Megara (locality S) and 0.2 mm a^{-1} at the Corinth isthmus (I) to 1.5–1.6 mm a^{-1} at Xylokastron and Derveni (C and

PHILOSOPHICAL TRANSACTIONS OF THE ROYAL SOCIETY A MATHEMATICAL, PHYSICAL & ENGINEERING SCIENCES

E) south of the central Gulf, where the active normal faulting is concentrated just offshore. The estimated maximum uplift over the past 0.9 million years also increases westward between these localities, from 80 m at Megara and 155 m at the Corinth isthmus to 1837 m at Mavron south of Derveni.

On the Perachora peninsula, I estimate 70, 180, and 360 m of uplift at localities H5, H10, and H13 by extrapolating from the palaeoshoreline evidence in table 3. Adding 600 m for the vertical slip on the Pisia and Skinos normal faults to this 70 m estimate of uplift at locality H5 predicts *ca.* 670 m of uplift in the mountain range in the central part of the peninsula, suggesting that the bulk of its *ca.* 1000 m of topography has developed in the past 0.9 million years. Comparison with the data from the Corinth isthmus indicates that the amount of uplift increases by *ca.* 530 m across the Loutraki fault, implying that it has slipped at least *ca.* 530 m on this timescale. This means that the vertical slip rate on this fault increased from a maximum of *ca.* 0.3 mm a^{-1} (1170 m/4.1 Ma) to a minimum of *ca.* 0.6 mm a^{-1} (530 m/0.9 Ma) around 0.9 million years ago.

The most abrupt structural relief has developed at Derveni (locality E). Allowing for the estimated *ca.* 200 m depth of the Gulf during the marine highstand *ca.* 0.9 million years ago, the earlier lake was *ca.* 120 m deep. Structural relief of *ca.* 120 m thus already existed across the *ca.* 10 km wide zone between the uppermost PGCB sediment surface at Mavron (assumed to be at shoreline level) and offshore of Derveni (assumed to be beneath 120 m of water). The present-day structural relief between these localities is *ca.* 3607 m, involving 1757 m of footwall topography, 1000 m of new sediment thickness, and *ca.* 850 m of water depth. The extra relief is thus 3487 m, partitioned with 1837 m of footwall uplift and 1650 m of hanging wall subsidence that represents the 1000 m of extra sediment plus the 650 m increase in water depth. This relief has developed by vertical slip on faults 2–4 in figure 5. I estimate that their slip has been partitioned with *ca.* 1057 m on fault 2, a minimum of *ca.* 1000 m on fault 3 (causing downthrow of top PGCB sediment from 900 m to −100 m), and *ca.* 1850 m on fault 4. This slip is partially cancelled by the observed *ca.* 200 m of southward back-tilting between faults 2 and 3, the required *ca.* 100 m of back-tilting between faults 3 and 4 (to drop top PGCB sediment from sea-level to −100 m), plus the additional 120 m of back-tilting to cancel the inferred *ca.* 120 m of northward depositional dip of the top PGCB sediment. The time-averaged differential rate of elevation change is thus almost 4 mm a^{-1}, with roughly equal footwall uplift and hanging-wall subsidence.

Between Corinth and Xylokastron, the onshore active normal faults complicate estimation of amounts of uplift. The uplift rate is *ca.* 0.3 mm a^{-1} south of Corinth town (locality A1), causing *ca.* 310 m uplift over the past 0.9 million years. South of Xylokeriza, the Earth's surface rises *ca.* 300 m across the Kenchriai fault (Vita-Finzi & King 1985) (figure 3). Assuming this offset has developed in 0.9 million years, it indicates a vertical slip rate of *ca.* 0.3 mm a^{-1}, so the uplift rate south of this fault is *ca.* 0.6 mm a^{-1} with *ca.* 600 m of uplift indicated over the past 0.9 million years. Moving south of Lecheon (locality A2), the uplift rate increases from *ca.* 0.1 to 0.4 then 0.6 mm a^{-1} in 7 km distance, as two active normal faults are crossed. The presence of the Kenchriai fault immediately south of this locality (figure 3) suggests a further increase in uplift rate to *ca.* 0.9 mm a^{-1}. The estimated uplift over the past 0.9 million years along this profile thus varies from 90 to 580 m. Moving southwest of Velon (locality B), the uplift rate increases from *ca.* 0.4 to 0.6 then 0.9 mm a^{-1} in 6 km distance, as two active normal faults are crossed. The terrace sequence again

PHILOSOPHICAL TRANSACTIONS OF THE ROYAL SOCIETY A MATHEMATICAL, PHYSICAL & ENGINEERING SCIENCES

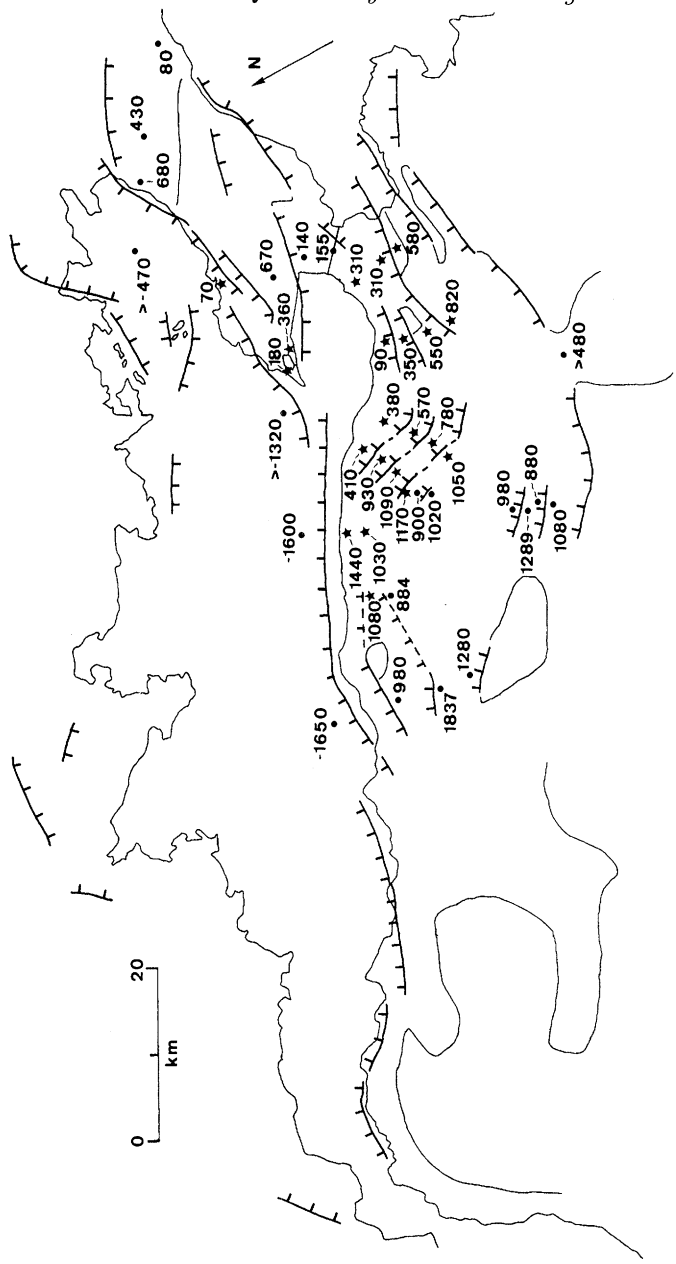

Figure 5. Summary map showing elevation changes in metres over the past 0.9 million years, obtained either from direct observation (sites marked by dots) or from the rates of elevation change in tables 3–5 (sites marked by stars). Normal faults in the vicinity of these localities, which affect local elevation changes, are also shown (with hanging-wall ticks).

ends just short of another active normal fault, identified by Vita-Finzi & King (1985), where *ca.* 300 m of displacement is estimated. With the estimated fault age again 0.9 million years, the uplift rate thus increases to *ca.* 1.2 mm a^{-1} farther south. The estimated uplift over the past 0.9 million years thus increases southwestward along this profile from 380 to 1050 m. Moving southwest of Kiaton (locality D), the uplift rate increases from *ca.* 0.4 to 0.5 to 1.0 to 1.2 then 1.4 mm a^{-1} in *ca.* 10 km distance, as four active normal faults (F12–F9) are crossed. The maximum uplift over the past 0.9 million ago is estimated as 1170 m in the footwall of fault F9. Immediately south

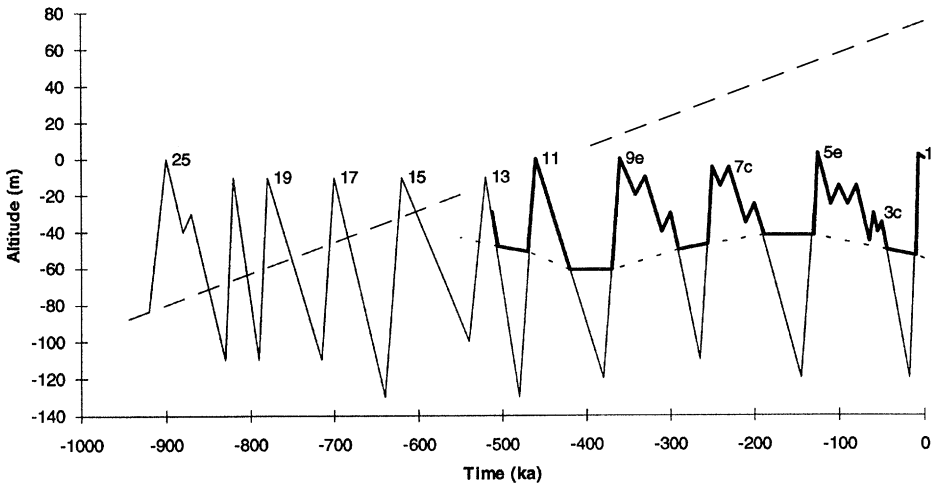

Figure 6. Summary of Gulf water level over the past 0.9 million years, labelled with the most important highstands. Thick solid line segments indicate estimated Gulf level since OIT stage 13. Thin solid lines indicate global sea-level before OIT stage 13 and at subsequent times when the Gulf has been lacustrine. Short dashes indicate the level of the Rion isthmus during marine highstands since OIT stage 13, assuming it has controlled the lake level in the Gulf during the intervening marine lowstands. Long dashes indicate the level of the Corinth isthmus, assuming it has risen uniformly from −80 m at 0.9 million years ago to +75 m at present. See text for discussion.

of these intensely faulted localities near the coast, uplift rates decrease as a result of back-tilting, which occurs at rates of up to *ca.* 10° Ma^{-1} from the evidence at Derveni, Xylokastron, Souli, and Psari.

Locality F *ca.* 20 km south of the Gulf indicates between 880 and *ca.* 1300 m of uplift over the past 0.9 million years, the variations being caused by normal faulting. Other normal faults in similar positions south of the Gulf are documented (e.g. the Agios Vasilios and Nemea faults in figure 3), which are also presumed active. These bound the PGCB and have evidently existed since local extension began around 5 million years ago. As a result of vertical slip on onshore normal faults, the maximum uplift south of the eastern Gulf is thus much greater than the amounts obtained by extrapolation from the uplift rates of the youngest marine terraces (figure 5).

Table 7 lists nomenclature for the sequence of late Pleistocene terraces in the Gulf, based on the Keraudren & Sorel (1987) scheme. Table 8 and figure 6 summarize the variations of Gulf level. The isthmus level at Rion has fluctuated between −40 and −60 m during the past 0.5 million years, with no clear long-term trend. The Corinth isthmus has instead risen roughly uniformly from −80 m during the past 0.9 million years. I thus tentatively suggest that both isthmi stood near −40 m during stage 16, and Gulf level was first unequivocally regulated at Rion during stage 14. During stages 17 and 15 (and perhaps also 13 and 11) the Gulf was thus apparently open at both ends.

5. Extension rates across the Gulf of Corinth

Vertical slip rates on normal faults in the Gulf of Corinth have been obtained from uplift rates and fault offsets. To estimate the associated extension rates I assume,

Table 7. *Terrace nomenclature for the Gulf of Corinth*

(Nomenclature for the known terraces in the Gulf of Corinth, D is the interpreted palaeo-water-level; t is the estimated age. I have adopted new notation for the lacustrine terraces (L), and have preserved as much as possible of the Keraudren & Sorel (1987) nomenclature for the marine terraces (M). This means redesignating the highest three marine terraces at Xylokastron (labelled 6.3, 7.1 and 7.3) as 7.1, 7.3 and 7.5 to be consistent with the other localities. Detail between OIT stages 25 and 12 is not yet resolved.)

				nomenclature			
				K&S (1987)			
stage	t/ka	D/m	type	Xylokastron	elsewhere	revised	name
1	7	+2	M			1	
2	45	−52	L			2L	
3a	50	−35	M	3.1		3.1	
3c	60	−30	M	3.3		3.3	
5a	80	−15	M	5.1	5.1	5.1	Agios Spiridon
5c	100	−15	M	5.3		5.3	Kounoukles
5e	125	0	M	5.5	5.5	5.5	New Corinth
6	190	−40	L	6.1		6L	
7a	200	−25	M	6.3	7.1	7.1	Tripos
7c	230	−5	M	7.1	7.3	7.3	Ancient Corinth
7e	250	−5	M	7.3	7.5	7.5	Temple
8	270	−50	L		8.1	8L	
9a	280	−30	M		8.5	8.5	
9c	330	−10	M		9.1	9.1	
9e	360	0	M		9.3	9.3	Nicoletto, etc.
10	430	−60	L			10L	
11	460	0	M			11.3	Veliniatika
12	>480	−50	L			12L	
19	*ca.* 730	*ca.* −20	M			19	Evrostini
25	900	0	M			25	
26	>900	−80	L			26L	

following Westaway & Kusznir (1993), that the surroundings to planar normal faults deform by distributed vertical simple shear. This means that the extension across any such fault equals its heave. The extension rate thus equals the rate of increase of heave, which is the vertical slip rate divided by the tangent of fault dip.

Westaway & Kusznir (1993) showed that a consequence of assuming vertical shear is that the tilt θ of an initially horizontal surface in the surroundings to a normal fault relates to the fault dip δ as

$$\tan(\theta) = \tan(\delta_0) - \tan(\delta), \tag{5.1}$$

Table 8. *Elevation changes of the floor of Rion strait*

(All information is from this study, except the 55 m present-day bathymetry, which is derived from the 30 fathom value in Heezen *et al.* (1966); one fathom equals 1.8288 m.)

stage	t/ka	D/m	source of information
12	480	51	Cliff A in the Corinth canal cut
10 (10L-1)	430	61	Cliff B in the Corinth canal cut
10 (10L-2)	380	61	Cliff C in the Corinth canal cut
8	270	47	terrace 8.1 at Lecheon
		50	terrace 8.1 at Velon
		>49	absence of stage 8 cliff in Corinth Canal cut
6	190	42	terrace 6.1 at Xylokastron
		>38	absence of stage 6 cliff in Corinth Canal cut
		>28	river terrace at Kiaton
1	0	55	present-day bathymetry

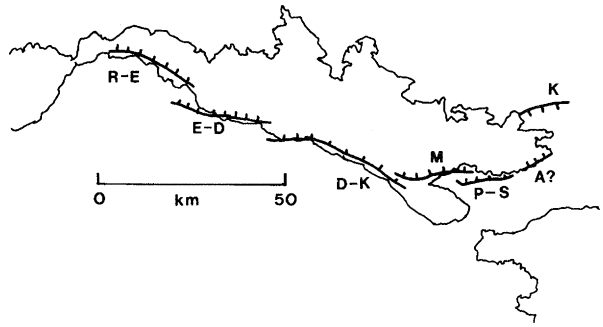

Figure 7. Summary map of the main normal fault segments controlling extension in the Gulf of Corinth over the past 0.9 million years. From west to east, these are the Rion-Egion (R-E), Egion-Derveni (E-D), Derveni-Kiaton (D-K), Milokopi (M), and Pisia/Skinos (P-S) faults. In the extreme east, it appears that the Alepochori fault (A) was most important during Pleistocene time, but the Kaparelli fault (K) has now taken over.

with δ_0 the initial dip of the fault. Differentiating (5.1) with respect to time t gives

$$\frac{\mathrm{d}\tan(\theta)}{\mathrm{d}t} = -\sec^2(\delta)\frac{\mathrm{d}\delta}{\mathrm{d}t} \tag{5.2}$$

as the relation between tilt rates of faults and horizontal surfaces. Many normal faults in the Gulf are steep. For instance, the Kaparelli fault dips at 60–70°; the Skinos and Pision fault scarps dip at 50–60° (Jackson *et al.* 1982). This means that the substantial (*ca.* 10° Ma^{-1}) tilt rates of young sediments do not require adjacent normal faults to tilt much. If a normal fault tilts from 67° to 65° dip, its surroundings will tilt by *ca.* 10°. With $\delta = 60$–$65°$, $\sec^2(\delta) \approx 4$–6, and tilt rates of faults are only *ca.* 1/4 to *ca.* 1/6 as large as those of adjacent beds.

Table 9 estimates rates of north-south extension across five representative profiles. The estimated extension rate is *ca.* 2 mm a^{-1} across the central Gulf; slightly less, *ca.* 1.5 mm a^{-1}, across its eastern parts. With a *ca.* 2 mm a^{-1} extension rate, the central part of the Gulf has thus extended by *ca.* 1.8 km over the past 0.9 million

years. With the present-day typical width of the Gulf plus PGCB *ca.* 50 km, their extension factor over the past 0.9 million years is thus *ca.* 50/48.2 or *ca.* 1.04.

From Kiaton westward, the most important normal faults bound the south coast of the Gulf (figure 7). West of the Perachora peninsula, the offshore part of the Milokopi fault becomes the most important, with *ca.* 1100 m of vertical slip estimated over the past 0.9 million years from Brooks & Ferentinos's (1984) seismic reflection profile. Moving east onto this peninsula, slip dies out on the Milokopi fault and builds up on the Pisia and Skinos faults, as is evident from the topography (Jackson *et al.* 1982). The most important active normal fault farther east during Holocene time has probably been at Kaparelli. However, as was noted by Leeder *et al.* (1991), if the early Holocene sea-level was less than +2 m, the Holocene vertical slip rate on the Alepochori fault around Psatha has also been non-zero.

There is no evidence for any major structural discontinuity on the coast between Xylokastron and Derveni, indicating that the Derveni-Kiaton fault in figure 7 is a single normal fault segment. Its *ca.* 35 km length is at the upper limit for the Aegean (Westaway 1993*a*, 1994*b*). West of Derveni, the coast steps abruptly northward; the same happens near Egion (Roberts & Jackson 1991). West of the Perachora peninsula the form of the Gulf is thus controlled by three major active normal fault segments (Rion-Egion, Egion-Derveni, and Derveni-Kiaton), each separated by a sideways step with some overlap.

Ori (1989) suggested that the present phase of extension in the Gulf of Corinth is coaxial about an axis to the west. If so, the extension rate is expected to increase linearly eastward. Table 9 suggests instead that extension rates are roughly uniform across the central Gulf, then decrease eastward. Near the western end of the Gulf the extension rate may well decrease westward, there being no evidence near Rion or along the Gulf of Patras for normal faulting on the scale needed to sustain 2 mm a^{-1} of extension. The apparent eastward decrease in the extension rate near the eastern end of the Gulf may to some extent reflect the omission of active normal faults south of the Agios Vasilios/Agionori area in figure 2, including faults bounding the Argos basin (figure 1) and others in the hills between this basin and the eastern PGCB (Papanastassiou *et al.* 1993), which arguably form part of the same system. One of these faults appears to have slipped in a major earthquake around 1190 B.C., damaging Mycenae and other nearby archaeological sites (Papanastassiou *et al.* 1993). However, the normal faults south of the eastern PGCB have been insufficiently studied to provide any robust estimate of the local extension rate. Nonetheless, if the overall extension rate were to maintain an eastward linear increase from say 0.5 mm a^{-1} at Rion to 2 mm a^{-1} at Xylokastron, it would need to be *ca.* 3 mm a^{-1} along a line between Navplion and the Psatha/Kaparelli area (figure 1). Such a high rate is unlikely, as the slow rates of vertical motion documented in the parts of this area that have been studied and the relatively subdued topography would seem to preclude the presence of normal faults with the slip rates needed to sustain such a high extension rate. The most rugged topography along this line is indeed around Psatha (figure 3), where the estimated vertical slip rate on the Alepochori fault has been no faster than *ca.* 0.2 mm a^{-1} at any stage during Quaternary time. The overall extension rate thus probably decreases both westward and eastward from a maximum of *ca.* 2 mm a^{-1} across the central part of the Gulf to substantially lower values – perhaps *ca.* 0.5 mm a^{-1} – at both its ends.

PHILOSOPHICAL TRANSACTIONS OF THE ROYAL SOCIETY A MATHEMATICAL, PHYSICAL & ENGINEERING SCIENCES

Table 9. *Extension rates*

(References are: 1, Ori (1989); 2, Doutsos & Piper (1990); 3, this study; 4, bathymetry in Heezen *et al.* (1966); 5, Vita-Finzi & King (1985); 6, Brooks & Ferentinos (1984); 7, Jackson *et al.* (1982). Y is vertical displacement; t is its age; U_y is vertical slip rate (either calculated as Y/t or estimated directly, in which case Y and t are not given); δ is estimated fault dip; U_x is rate of increase of heave, calculated as $U_y \cot \delta$; V_e is extension rate across each cross section, calculated as the sum of U_x values. I assume ages of 5 million years for the F1, Nemea and Agios Vasilios normal faults, which bound the PGCB, and 3 million years for the Almiri fault within the PGCB. Faults F2 and F3 near Psari are discussed in the text. Their estimated displacements are the fractions over the past 0.9 million years. The south-dipping South Alkyonides fault and north-dipping north Alkyonides fault bound the Alkyonides islands in the western Alkyonides Gulf (figure 5). Their vertical displacements are interpreted from the bathymetry. The south-dipping Akra Aga and Makronisos fault bound the north coast of the Gulf west of Paralia and between Pelagia and Aliki (figures 1 and 5).)

fault	ref.	Y/m	t/ka	U_y/(mm a^{-1})	δ/deg	U_x/(mm a^{-1})	V_e/(mm a^{-1})
(i) *Derveni*							
all faults combined	1	3500	900	3.9	*ca.* 65	1.8	1.8
(ii) *Psari–Xylokastron* (*ca.* 20 km *east of* (i))							
fault F1	2	700	5000	0.1	*ca.* 65		
fault F2	2	200	900	0.2	*ca.* 65		
fault F3	2	300	900	0.3	*ca.* 65	0.3	
coastal footwall uplift on offshore fault	3			1.6			
offshore subsidence	4	1800	900	2.0	*ca.* 65	1.7	2.0
(iii) *Nemea–Souli – west of Kiaton* (*ca.* 8 km *east of* (ii))							
Nemea fault	5	500	5000	0.1			
fault F8	2			0.1			
fault F9	2			0.1			
fault F10	2			0.2			
fault F11	2			0.6	65	0.5	
fault F12	2			0.1			
coastal footwall uplift on offshore fault	3			0.4			
offshore subsidence	4	1600	900	1.8	65	1.1	1.6
(iv) *Agios Vasilios – Penteskoufi – west of Lecheon – west of Perachora peninsula* (8 km *east of* (iii))							
Agios Vasilios fault	5	700	5000	0.1	65	0.1	
Akrocorinth fault	3			0.2	65	0.1	
Lecheon fault (upper limit)	3			0.3	65	0.1	
normal fault at locality P1 (Milokopi fault)	6	1200	900	1.3	55	0.9	
Akra Aga fault	5	600	900	0.7	65	0.3	1.5

Table 9. *Cont.*

fault	ref.	Z/m	t/ka	U_z/(mm a^{-1})	δ/deg	U_x/(mm a^{-1})	V_e/(mm a^{-1})
(v) *East of Agionori – Corinth – Pisia* (12 km *east of* (iv))							
Agios Vasilios fault	5	500	5000	0.1	65		
Almiri fault	5	200	3000	0.1	65		
Kenchriai fault	5	300	900	0.3	65	0.2	
Loutraki fault	3			0.6	55	0.4	
Pisia fault	3	300	900	0.3	55	0.2	
Skinos fault	3	300	900	0.3	55	0.2	
South Alkyonides fault	4	300	900	0.3	65		
North Alkyonides fault	4	300	900	0.3	65	0.3	
Makronisos fault	5	300	900	0.3	65	0.1	1.4

6. Causes of elevation change around the Gulf of Corinth

Most topography and bathymetry in the Gulf has thus formed during the past 0.9 million years, and is associated with normal faulting. For the 60 km by 30 km central Gulf, the turbidite thickness is uniformly *ca.* 1 km for the *ca.* 10 km wide abyssal plain (Brooks & Ferentinos 1984); it then tapers northward to zero over *ca.* 10 km distance. Its volume is thus *ca.* 900 km^3. From Heezen *et al.* (1966) I estimate typical water depths of 800, 500 and 100 m in each of these *ca.* 10 km wide swathes, or *ca.* 500 m on average; the total water volume is thus also *ca.* 900 km^3.

The horizontal lithostatic pressure difference δp driving lower-crustal flow can be estimated as

$$\delta p = 16\eta LV/W^2 \tag{6.1}$$

(Westaway 1994*a*), where W is the thickness of the lower-crustal channel, η is its viscosity, L is the width of the extensional basin, and V is the maximum velocity of the flow. V can be estimated as

$$V = 3Q/2WJ, \tag{6.2}$$

where Q is the lower-crustal volume flux and J is the along-strike length of the basin. To estimate Q from elevation changes, it is necessary to take isostatic compensation into account.

(*a*) *Isostatic response of the central Gulf of Corinth to outward lower-crustal flow*

Let T_c and T_c' denote the thickness of crustal basement beneath the Gulf 0.9 million years ago and at present. If the Gulf has extended by factor β on this timescale, and has lost crustal thickness E by outward lower-crustal flow, then

$$T_c' = T_c/\beta - E. \tag{6.3}$$

Let T_w and T_s denote the thickness of water and sediment that have accumulated in the Gulf over the past 0.9 million years, and let U_M denote the uplift of the Moho to maintain isostatic equilibrium, such that

$$T_c = T_w + T_s + T_c' + U_M. \tag{6.4}$$

Isostatic equilibrium requires that

$$T_c\rho_c = T_w\rho_w + T_s\rho_s + T'_c\rho_c + U_M\rho_m, \tag{6.5}$$

where ρ_w, ρ_s, ρ_c and ρ_m are the densities of water, sediment, crustal basement, and mantle lithosphere. Rearranging (6.3)–(6.5) thus gives

$$E = T_w\frac{\rho_m - \rho_w}{\rho_m - \rho_c} + T_s\frac{\rho_m - \rho_s}{\rho_m - \rho_c} - T_c(1 - 1/\beta). \tag{6.6}$$

With ρ_m, ρ_c, ρ_s, and ρ_w 3200, 2700, 2200 and 1000 kg m^{-3}, respectively, $T_w = 0.5$ km, $T_s = 0.5$ km (both averaged across the Gulf), $T_c = 30$ km and $\beta = 1.04$, the three terms in (6.6) are 2.2, 1.0, and −1.2 km. The typical crustal thickness E lost by outward flow is thus 2.0 km. For the central *ca.* 60 km of the Gulf, the estimated crustal outflow over the past 0.9 million years is thus $2 \times 30 \times 60$ or 3600 km^3, so Q is *ca.* 4×10^6 m^3 a^{-1}. W can be estimated as no less than *ca.* 20 km given the minimum *ca.* 32 km crustal thickness for central Greece (Makris & Vees 1977) and the thickness (less than *ca.* 10 km) of the brittle layer indicated by the seismicity (Taymaz *et al.* 1991). With $W = 20$ km and $J = 60$ km, the maximum flow velocity V is estimated as *ca.* 5 mm a^{-1}. With $L = 30$ km, δp (time-averaged over the past 0.9 million years) is *ca.* 0.2 MPa for η 10^{18} Pa s (or, say, *ca.* 0.6 MPa for η 3×10^{18} Pa s or *ca.* 2 MPa for η 10^{19} Pa s). With W larger, say 25 km, δp for each value of η would be only *ca.* 64% of the above values.

Rearranging (6.4)–(6.6) gives

$$\frac{T_w}{T_s} = \frac{U_M}{T_s}\frac{\rho_m - \rho_c}{\rho_c - \rho_w} - \frac{\rho_c - \rho_s}{\rho_c - \rho_w}, \tag{6.7}$$

which simplifies, using my parameters (where $\rho_m - \rho_c = \rho_c - \rho_s$) to $T_w/T_s = \frac{5}{17}(U_M/T_s - 1)$. The roughly equal water and sediment thickness in the Gulf thus means that the Moho uplift $U_M \approx \frac{22}{5} \times T_s$. Using (6.4), $U_M = T_c - T'_c - T_w - T_s$, or $3.2 - 0.5 - 0.5$ km, giving *ca.* 2.2 km. The spatially averaged and time averaged Moho uplift rate is thus *ca.* 2.2 km/0.9 Ma, or *ca.* 2.4 mm a^{-1}.

(*b*) *Isostatic response of localities surrounding the Gulf of Corinth to inward lower-crustal flow*

Suppose that 0.9 million years ago a locality near the Gulf was covered with a thickness T_s of sediment, which has since eroded, and had a crustal basement thickness T_c. Suppose that the subsequent influx of lower-crustal material with thickness F has caused isostatic uplift U_c of the uppermost crustal basement and subsidence S_M of the Moho. Thus

$$T_s = F - U_c - S_M. \tag{6.8}$$

Isostatic equilibrium requires

$$T_s\rho_s = (F - U_c)\rho_c - S_M\rho_m. \tag{6.9}$$

Solving (6.8)–(6.9) gives

$$F - U_c = T_s\frac{\rho_m - \rho_s}{\rho_m - \rho_c}. \tag{6.10}$$

In a locality with no erosion ($T_s = 0$), $F = U_c$; the lower-crustal influx thus equals the uplift of the Earth's surface. The *ca.* 1.1 km uplift near Psari, where preservation of the uppermost PGCB sediment indicates that little or no erosion has occurred,

thus indicates $F \approx 1.1$ km. If this were characteristic of the whole *ca.* 20×60 km^2 exposed area of the PGCB south of the central Gulf, an influx of *ca.* 1300 km^3 would be required. If instead this exposed area of the PGCB were eroding uniformly and supplying all the 900 km^3 of Gulf sediment, conservation of volume requires $T_s \approx 0.75$ km; from (6.10), $F - U_c$ is thus *ca.* 1.5 km. Dividing the *ca.* 3600 km^3 maximum influx from beneath the Gulf by the dimensions of the PGCB gives $F \approx 3$ km and thus $U_c \approx 1.5$ km. Typical uplift by 1.5 km is thus expected in the PGCB if it has accommodated all the influx from beneath the Gulf and has eroded uniformly. However, the area south of the Gulf now occupied by river valleys and mountains that rise above the remaining PGCB sediment is *ca.* 2/3 of the total. If substantial erosion is instead restricted to these localities, a spatial average of *ca.* 1.1 km of erosion is required to supply all the sediment in the central Gulf.

The main constraints are thus, first, the volume flux required to support the uplift south of the Gulf cannot exceed the outflow from beneath the Gulf. Second, the maximum uplift of the PGCB caused by lower-crustal influx is near the *ca.* 1.1–1.8 km observed in localities such as Psari and Karia, which have not eroded. Third, the maximum spatially averaged erosion is *ca.* 0.75 km. My preferred solution regards typical amounts of uplift and erosion as tapering both eastward and westward away from the central Gulf. I regard all the turbiditic sediment within the Gulf as derived from erosion of the PGCB, and regard the uplift as tapering southward from the high values within the PGCB to values near zero *ca.* 40 km south of the Gulf. I regard the average uplift of this peripheral zone as roughly half that of the PGCB, say 500 m. From (12) this requires *ca.* 600 km^3 of influx; the remaining *ca.* 3000 km^3 having uplifted the PGCB. From (6.10), the influx to beneath the PGCB requires $F = 2.5$ km. With $F - U_c = 1.5$ km (see above), U_c (spatially averaged across the PGCB) is estimated as 1.0 km. The required time-averaged erosion rate is thus 0.75 km/0.9 Ma or *ca.* 0.8 mm a^{-1} spatially averaged across the PGCB, or *ca.* 1.3 mm a^{-1} for the *ca.* 2/3 of it that is eroding.

(*c*) *Summary*

The two phases of evolution of the Gulf of Corinth (the PGCB and the modern basin) are explained by a reversal in the sense of lower-crustal flow, from inward to outward, around 0.9 million years ago. The absence of substantial subsidence despite prolonged extension before 0.9 million years ago suggests inward lower-crustal flow, although δp may have been only marginally negative. The marine incursion 0.9 million years ago flooded the Corinth isthmus to a depth of $h \approx 80$ m, raising the lithostatic pressure throughout the Gulf by *ca.* 0.8 MPa (calculated as $\rho_w g h$ where $g \approx 10$ m s^{-2} is the acceleration due to gravity). The typical estimated subsequent time-averaged outward pressure head has indeed been *ca.* 0.8 MPa for a range of possible values of W and η, and implies $\eta < 3 \times 10^{18}$ Pa s.

Isostatic compensation of this *ca.* 80 m water load would require outflow of *ca.* 30 m thickness of the lower crust from beneath the Gulf, which would uplift its surroundings to the south. This uplift of unconsolidated sediment would create an unstable landscape, susceptible to rapid erosion. The resulting sediment load to the Gulf would require more outflow and hence more uplift of its southern flank. A self-sustaining cycle of erosion, sediment loading, lower-crustal flow, and uplift, was thus created, which will probably last until all the PGCB sediment is eroded into the Gulf. The elevation change of any other locality in and around the Gulf depends on

PHILOSOPHICAL TRANSACTIONS OF THE ROYAL SOCIETY A MATHEMATICAL, PHYSICAL & ENGINEERING SCIENCES

whether there has been net inflow or outflow beneath it. For instance, the uplift of the Corinth isthmus can be interpreted as indicating local inflow.

A similar cycle has probably occurred on a smaller scale between the Alkyonides Gulf and the Megara basin. From (6.6), compensation of the *ca.* 180 m of sediment that results from erosion of this basin and the *ca.* 350 m of water covering the *ca.* 50 km^2 abyssal plain in this Gulf will uplift this *ca.* 100 km^2 basin and an equal surrounding area by *ca.* 300 m, or by between *ca.* 600 m in the NW and zero in the SE. The uplift and southeastward present-day tilt of this basin thus probably result from this process. The decrease in uplift rate of the northwestern part of the Megara basin since the early part of late Pleistocene time suggests that the available sediment supply rapidly became exhausted.

(*d*) *Wider implications*

Normal fault zones in other coastal parts of the Aegean region also contain uplifted Neogene basins in the footwalls of active normal faults (Roberts & Jackson 1991). This characteristic geomorphology may be caused by the sequence of processes suggested for the Gulf of Corinth. First, global sea-level fell in early Pleistocene time, in some cases leaving lacustrine basins at lower elevation. Second, continuing extension and the associated footwall uplift gradually raised footwall localities in the flanks of extensional basins. Third, the central part of each basin became flooded *ca.* 0.9 million years ago, but the flanking localities remained above the new water level. Finally, the lithostatic pressure anomaly caused by this water load drove outward lower-crustal flow, which uplifted the flanking localities more and led to erosion. The resulting sediment load will sustain this sense of lower-crustal flow, which will sustain the uplift of the flanking localities, until the uplifted basin has fully eroded. For instance, the *ca.* 300 m elevation of Plio-Pleistocene basins north of the Gulf of Corinth (Roberts & Jackson 1991) may result from compensation of outflow from beneath other marine basins offshore of central Greece.

7. Conclusions

All terraces in the Gulf of Corinth identified by Keraudren & Sorel (1987) are real. However, some are lacustrine, not marine. In many localities these terraces are cut by active normal faults, such that the oldest terraces uplift fastest as a result of relative footwall uplift. The maximum uplift rates south of the Gulf are thus above 1 mm a^{-1} for much of its length, much higher than the rates indicated by the lowest terraces, with back-tilting at up to *ca.* 10° Ma^{-1} inferred from the southward tapering in uplift rate. Indicators of Holocene elevation change from archaeological sites and shorelines are reliable. Some localities show complex Holocene elevation changes, which are interpreted as the combined effect of a limited number of major normal-faulting earthquakes. Allowing for the extension on normal faults up to *ca.* 20 km south of the Gulf, the estimated extension rate across its central part is *ca.* 2 mm a^{-1}, roughly half the *ca.* 4 mm a^{-1} rate of differential elevation change across its south coast. The estimated extension rate tapers slightly east to *ca.* 1.5 mm a^{-1} with smaller values probable at the eastern extremity of the Gulf, and presumably also tapers westward. As was noted by Ori (1989), the Gulf changed abruptly around 0.9 million years ago from a lacustrine environment with slow sedimentation and gentle relief to its present environment with dramatic erosion and sedimentation, and abrupt fault-controlled topopography. The maximum uplift south the Gulf over

PHILOSOPHICAL TRANSACTIONS OF THE ROYAL SOCIETY A MATHEMATICAL, PHYSICAL & ENGINEERING SCIENCES

the past 0.9 million years is *ca.* 1837 m; the maximum subsidence of its interior is *ca.* 1650 m.

To explain this dramatic change, it is suggested that the *ca.* 80 m of water loading when the lacustrine basin was flooded by the sea 0.9 million years ago caused a positive lithostatic pressure anomaly at the base of the brittle upper crust. This caused outflow of the lower crust to beneath the Plio-Pleistocene basin farther south. This uplifted this basin, triggering its dramatic erosion. The resulting sediment load in the Gulf has maintained the lithostatic pressure anomaly, which will persist until this uplifting basin has eroded. This process is estimated to have uplifted the *ca.* 20 km wide basin south of the the *ca.* 60 km long central Gulf by 1 km on average, plus a *ca.* 20 km wide zone farther south by an average of *ca.* 500 m. This outward lower-crustal flow explains the uplift of the Corinth isthmus and other hanging-wall localities.

I thank John Dewey and Denis Sorel for their comments on an earlier version of this manuscript.

References

Bentham, P., Collier, R. E. Ll., Gawthorpe, R. L., Leeder, M. R., Prossor, S. & Stark, C. 1991 Tectono-sedimentary development of an extensional basin: the Neogene Megara basin, Greece. *J. Geol. Soc. Lond.* **148**, 923–934.

Billiris, H., Paradissis, D., Veis, G., England, P., Featherstone, W., Parsons, B., Cross, P., Rands, P., Rayson, M., Sellers, P., Ashkenazi, V., Davison, M., Jackson, J. & Ambraseys, N. 1991 Geodetic determination of tectonic deformation in central Greece from 1900 to 1988. *Nature* **350**, 124–129.

Brooks, M. & Ferentinos, G. 1984 Tectonics and sedimentation in the Gulf of Corinth and the Zakynthos and Kefallinia channels, western Greece. *Tectonophys.* **101**, 25–54.

Brooks, M., Clews, J. E., Melis, N. S. & Underhill, J. R. 1988 Structural development of Neogene basins in western Greece. *Basin Res.* **1**, 129–138.

Carydis, P. G., Tilford, N. R., Brandow, G. E. & Jirsa, J. O. 1982 The central Greece earthquakes of February–March 1981. Report CETS-CND-018 of the Earthquake Engineering Research Institute, Berkeley, California. Washington, DC: National Academy Press.

Chappell, J. & Shackleton, N. J. 1986 Oxygen isotopes and sea-level. *Nature* **324**, 137–140.

Collier, R. E. Ll. 1990 Eustatic and tectonic controls upon Quaternary coastal sedimentation in the Corinth basin, Greece. *J. Geol. Soc. Lond.* **147**, 301–314.

Collier, R. E. Ll. & Dart, C. J. 1991 Neogene to Quaternary rifting, sedimentation and uplift in the Corinth basin, Greece. *J. Geol. Soc. Lond.* **148**, 1049–1065.

Collier, R. E. Ll., Leeder, M. R. & Maynard, J. R. 1990 Transgressions and regressions: a model for the influence of tectonic subsidence, deposition and eustasy, with application to Quaternary and Carboniferous examples. *Geol. Mag.* **127**, 117–128.

Collier, R. E. Ll., Leeder, M. R., Rowe, P. J. & Atkinson, T. C. 1992 Rates of tectonic uplift in the Corinth and Megara basins, central Greece. *Tectonics* **11**, 1159–1167.

Comninakis, P. E. & Papazachos, B. C. 1982 A catalogue of historical earthquakes in Greece and surrounding area, 479 B.C.–1900 A.D. University of Thessaloniki Geophysical Laboratory publication 5.

Depéret, C. 1913 Observations sur l'histoire géologique pliocene et quaternaire du golfe et de l'isthme de Corinthe. *C.R. Hebd. Séanc. Acad. Sci. Paris* **156**, 426–431, 659–663, 1048–1052.

Doutsos, T. & Piper, D. J. W. 1990 Listric faulting, sedimentation, and morphological evolution of the Quaternary eastern Corinth rift, Greece: first stages of continental rifting. *Geol. Soc. Am. Bull.* **102**, 812–829.

Doutsos, T., Kontopoulos, N. & Ferentinos, G. 1985 Das westliche Ende des Korinth-Grabens. *N. Jahrb. Geol. Paläontol. Monatshefte 1985*, pp. 652–666.

PHILOSOPHICAL TRANSACTIONS OF THE ROYAL SOCIETY A MATHEMATICAL, PHYSICAL & ENGINEERING SCIENCES

Dufaure, J. J., Keraudren, B. & Sébrier, M. 1975 Les terrasses de Corinthe: chronologie et déformations. *C.R. Acad. Sci. Paris*, Sér. D **281**, 1943–1945.

Dufaure, J. J. & Zamanis, A. 1980 Styles néotectoniques et étagements de niveaux marins sur un segment d'arc insulaire, le Péloponnèse. In *Proc. colloquium on Niveaux Marins et Tectonique Quaternaire dans l'Aire Méditeranéenne*, Université Paris I. Paris: CNRS.

Ferentinos, G., Papatheodorou, G. & Collins, M. B. 1988 Sediment transport processes on an active submarine fault escarpment: Gulf of Corinth, Greece. *Mar. Geol.* **83**, 43–61.

Fink, R. & Schröder, B. 1975 Facts indicating a Holocene high sea-level near the isthmus of Corinth. *N. Jahrb. Geol. Paläontol. Monatshefte 1975*, pp. 265–270 (in German with English abstract).

Flemming, N. C. 1965 Form and relation to present sea-level of Pleistocene marine erosion features. *J. Geol.* **73**, 799–811.

Flemming, N. C. 1968 Derivation of Pleistocene marine chronology from morphometry of erosion profiles. *J. Geol.* **76**, 280–296.

Flemming, N. C. 1978 Holocene eustatic changes and coastal tectonics in the northeast Mediterranean: implications for models of crustal consumption. *Phil. Trans. R. Soc. Lond.* A **289**, 405–458.

Flemming, N. C. & Webb, C. O. 1986 Tectonic and eustatic coastal changes during the last 10,000 years derived from archaeological data. *Z. Geomorph. N.F.* Suppl. **62**, 1–29.

Freyberg, B. von 1973 Geologie des Isthmus von Korinth. *Erlanger Geol. Abhandlungen* **95**, 1–183.

Ghisetti, F. 1992 Fault parameters in the Messina Strait (southern Italy) and relations with the seismogenic source. *Tectonophys.* **210**, 117–133.

Hearty, P. J., Miller, G. H., Stearns, C. E. & Szabo, B. J. 1986 Aminostratigraphy of Quaternary shorelines in the Mediterranean basin. *Geol. Soc. Am. Bull.* **97**, 850–858.

Heezen, B. C., Ewing, M. & Johnson, G. L. 1966 The Gulf of Corinth floor. *Deep-Sea Res.* **13**, 381–411.

Herforth, A. & Richter, D. K. 1979 A Pleistocene step fault system covered by marine terraces, Perachora Peninsula near Korinthos (Greece). *N. Jahrb. Geol. Paläont. Abhandlungen* **159**, 1–13 (in German with English abstract).

Herforth, A., Schröder, B. & Theodoropoulos, D. 1971 Zur jungpleistozänen und Holozänen Küsten-morphologie zwischen Korinth und sud-Attika. *Bull. Geol. Soc. Greece* **8**, 194–198.

Jackson, J. A., Gagnepain, J., Houseman, G., King, G. C. P., Papadimitriou, P., Soufleris, C. & Virieux, J. 1982 Seismicity, normal faulting, and the geomorphological development of the Gulf of Corinth (Greece): the Corinth earthquakes of February and March 1981. *Earth. Planet. Sci. Lett.* **57**, 377–397.

Kelletat, D., Kowalczyk, G. Schröder, B. & Winter, K.-P. 1976 A synoptic view on the neotectonic development of the Peloponnesian coastal region. *Z. Deutsche Geol. Ges.* **127**, 447–465.

Kelletat, D., Kowalczyk, G., Schröder, B. & Winter, K.-P. 1978 Neotectonics in the Peloponnesian coastal regions. In *Alps, Apennines, Hellenides: geodynamic investigations along geotraverses by an international group of geoscientists. Inter-Union Commission of Geodynamics Sci. Rep. 38* (ed. H. Closs, D. Roeder & K. Schmidt), pp. 512–518. Stuttgart: Schweitzerbart.

Keraudren, B. 1970 Les formations quaternaires marines de la Grèce. *Bull. Mus. Anthrop. Préhist., Monaco* **16**, 5–153.

Keraudren, B. 1971 Les formations quaternaires marines de la Grèce. *Bull. Mus. Anthrop. Préhist., Monaco* **17**, 87–169.

Keraudren, B. 1972 Les formations quaternaires marines de la Grèce. *Bull. Mus. Anthrop. Préhist., Monaco* **18**, 245–279.

Keraudren, B. & Sorel, D. 1987 The terraces of Corinth (Greece): a detailed record of eustatic sea-level variations during the last 500,000 years. *Mar. Geol.* **77**, 99–107.

Kinder, H. & Hilgemann, W. 1974 *The Penguin atlas of world history*, vol. 1. *From the beginning to the eve of the French Revolution.* New York: Penguin Books.

King, G. C. P., Stein, R. S. & Rundle, J. B. 1988 The growth of geological structures by repeated earthquakes. 1. Conceptual framework. *J. Geophys. Res.* **93**, 13307–13318.

PHILOSOPHICAL TRANSACTIONS OF THE ROYAL SOCIETY A MATHEMATICAL, PHYSICAL & ENGINEERING SCIENCES

Kruse, S., McNutt, M., Phipps-Morgan, J., Royden, L. & Wernicke, B. 1991 Lithospheric extension near Lake Mead, Nevada: a model for ductile flow in the lower crust. *J. Geophys. Res.* **96**, 4435–4456.

Leeder, M. R. & Jackson, J. A. 1993 The interaction between normal faulting and drainage in active extensional basins, with examples from the western United States and central Greece. *Basin Res.* **5**, 79–102.

Leeder, M. R., Seger, M. J. & Stark, P. 1991 Sedimentation and tectonic geomorphology adjacent to major active and inactive normal faults, southern Greece. *J. Geol. Soc. Lond.* **148**, 331–343.

Le Pichon, X. & Angelier, J. 1981 The Aegean Sea. *Phil. Trans. R. Soc. Lond.* A **300**, 357–372.

Le Pichon, X., Chamot-Rooke, N., Noomen, R. & Veis, G. 1994 Kinematics of Anatolia-Aegea with respect to stable Europe based on a combination of SLR and geodetic measurements over 80 years. *C.R. Acad. Sci. Paris*, Sér. II **318**, 1387–1393 (in French with English summary).

Le Pichon, X., Chamot-Rooke, N., Lallement, S., Noomen, R. & Veis, G. 1995 Geodetic determination of the kinematics of central Greece with respect to Europe: implications for eastern Mediterranean tectonics. *J. Geophys. Res.* **100**, 12675–12690.

Makris, J. & Vees, R. 1977 Crustal structure of the central Aegean Sea and the islands of Evia and Crete, Greece, obtained by refractional seismic experiments. *J. Geophys.* **42**, 329–341.

Mariolakos, I. & Stiros, S. C. 1987 Quaternary deformation of the Isthmus and Gulf of Corinthos (Greece). *Geology* **15**, 225–228.

Mitzopoulos, M. K. 1933 Le Quaternaire marin (Tyrrhénien) dans la presqu'île de Pérachora. *Praktika Akad. Athens* **8**, 286–292.

Myrianthis, M. 1984 Graben formation and associated seismicity in the Gulf of Korinth (central Greece). In *The Geological evolution of the Eastern Mediterranean* (ed. J. E. Dixon & A. H. F. Robertson). *Spec. Publ. Geol. Soc. Lond.* **17**, 701–707.

Ori, G. G. 1989 Geologic history of the extensional basin of the Gulf of Corinth (?Miocene–Pleistocene), Greece. *Geology* **17**, 918–921.

Papanastassiou, D., Maroukian, H. & Gaki-Papanastassiou, K. 1993 Morphotectonic and archaeological observations in the eastern Argive Plain (eastern Peloponnese, Greece) and their palaeoseismological implications. *Z. Geomorph. N.F. Suppl.* **94**, 95–105.

Paskoff, R. P. & Sanlaville, P. 1981 Tyrrhenian deposits and neotectonics at Monastir, Tunisia. *Z. Geomorph. N.F. Suppl.* **40**, 183–192.

Pirazzoli, P. A., Stiros, S. C., Arnold, M., Laborel, J., Laborel-Deguen, F. & Papageorgiou, S. 1994 Episodic uplift deduced from Holocene shorelines in the Perachora peninsula, Corinth area, Greece. *Tectonophys.* **229**, 201–209.

Richter, D. K., Herforth, A. & Ott, E. 1979 Brackish blue-green algal bioherms composed by Rivularia haematites in Pleistocene deposits of the Perachora Peninsula near Korinthos (Greece). *N. Jahrb. Geol. Paläontol. Abhandlungen* **159**, 14–40 (in German with English abstract).

Roberts, G. & Stewart, I. 1994 Uplift, deformation and fluid involvement within an active normal fault zone in the Gulf of Corinth, Greece. *J. Geol. Soc. Lond.* **151**, 531–541.

Roberts, G., Gawthorpe, R. & Stewart, I. 1993 Surface faulting within active normal fault zones: examples from the Gulf of Corinth fault system, central Greece. *Z. Geomorph. N.F. Suppl.* **94**, 303–328.

Roberts, S. C. 1988 Active normal faulting in central Greece and western Turkey. Ph.D. thesis, Cambridge University.

Roberts, S. C. & Jackson, J. A. 1991 Active normal faulting in central Greece: an overview. In *The geometry of normal faults* (ed. A. M. Roberts, G. Yielding & B. Freeman). *Spec. Publ. Geol. Soc. Lond.* **56**, 125–142.

Sauvage, J. & Dufaure J.-J. 1976 Sur une flore pré-tiglienne dans la série marno-conglomératique corinthienne (Péloponèse, Grèce). *C.R. Acad. Sci. Paris*, Sér. D **282**, 687–690.

Schröder, B. 1970 Über mittel- und jung-pleistozäne Meeres-Hochstände der Landenge von Korinth. *N. Jahrb. Geol. Paläontol. Monatshefte 1970*, pp. 27–33 (in German with English abstract).

Schröder, B. 1975 Comments on Quaternary marine terraces in the NE Peloponnesos, Greece. *N. Jahrb. Geol. Paläontol. Abhandlungen* **149**, 148–161 (in German with English abstract).

PHILOSOPHICAL TRANSACTIONS OF THE ROYAL SOCIETY A MATHEMATICAL, PHYSICAL & ENGINEERING SCIENCES

Sébrier, M. 1977 Tectonique récente d'une transversale à l'Arc Egéen: Le Golfe de Corinthe et ses régions périphériques. Ph.D. thesis, Université de Paris-Sud, Centre d'Orsay.

Shackleton, N. J. 1987 Oxygen isotopes, ice volume and sea-level. *Quat. Sci. Rev.* **6**, 183–190.

Shackleton, N. J., Berger, A. & Peltier, W. R. 1990 An alternative astronomical calibration of the lower Pleistocene timescale based on ODP site 677. *Trans. R. Soc. Edinb. Earth Sci.* **81**, 251–261.

Stiros, S. C. 1986 Geodetically controlled taphrogenesis in backarc environments: three examples from central and northern Greece. *Tectonophys.* **130**, 281–288.

Symeonides, N., Theodorou, G. Schütt, H. & Velitzelos, E. 1987 Paleontological and stratigraphic observations in the area of Achaia and Etoloakarnania (W. Greece). *Ann. géol. des pays helleniques* **38**, 317–353.

Taymaz, T., Jackson, J. & McKenzie, D. 1991 Active tectonics of the north and central Aegean Sea. *Geophys. J. Int.* **106**, 433–490.

Valensise, G. & Pantosti, D. 1992 A 125 kyr-long geological record of seismic source repeatability: the Messina Straits (southern Italy) and the 1908 earthquake (Ms 7 1/2). *Terra Nova* **4**, 472–483.

Vita-Finzi, C. 1986 *Recent earth movements: an introduction to neotectonics*. Orlando, FL: Academic Press.

Vita-Finzi, C. 1987 ^{14}C deformation chronologies in coastal Iran, Greece, and Jordan. *J. Geol. Soc. Lond.* **144**, 553–560.

Vita-Finzi, C. & King, G. C. P. 1985 The seismicity, geomorphology and tectonic evolution of the Corinth area of Greece. *Phil. Trans. R. Soc. Lond.* A **314**, 379–407.

Wernicke, B. 1990 The fluid crustal layer and its implications for continental dynamics. In *Exposed cross-sections of the continental crust* (ed. M. H. Salisbury & D. M. Fountain), pp. 509–544. Norwell, MA: Kluwer.

Westaway, R. 1993*a* Neogene evolution of the Denizli region of western Turkey. *J. Struct. Geol.* **15**, 37–53.

Westaway, R. 1993*b* Quaternary uplift of southern Italy. *J. Geophys. Res.* **98**, 21741–21772.

Westaway, R. 1994*a* Reevaluation of extension in the Pearl River Mouth basin, South China Sea: implications for continental lithosphere deformation mechanisms. *J. Struct. Geol.* **16**, 823–838.

Westaway, R. 1994*b* Evidence for dynamic coupling of surface processes with isostatic compensation in the lower crust during active extension of western Turkey. *J. Geophys. Res.* **99**, 20203–20223.

Westaway, R. & Kusznir, N. J. 1993 Fault and bed 'rotation' during continental extension: block rotation or vertical shear? *J. Struct. Geol.* **15**, 153–170; 1391 (correction).

Westaway, R. & Smith, R. B. 1989 Strong ground motion in normal-faulting earthquakes. *Geophys. J.* **96**, 529–559 + microfiches G7 96/1-1 and G7 96/1-2.

Williams, D. F., Thunell, R. C., Tappa, E., Rio, D. & Raffi, I. 1988 Chronology of the Pleistocene oxygen isotope record: 0–1.88 m.y. BP. *Paleogeogr. Paleoclimatol. Paleoecol.* **64**, 221–240.

Zeuner, F. E. 1956 The three 'Monastirian' sea-levels. In *Proc. 4th INQUA Congress, Rome 1953*, pp. 547–553.

Received 17 May 1995; accepted 25 May 1995